Key Points:

- Thrace Basin is a late Eocene - Oligocene clastic basin with >90% of the sedimentary fill deposited in the early Oligocene at rates of 1.0 km/my
- The main subsidence in the Thrace Basin (34-28 Ma) was coeval with the exhumation of the northern Rhodope Complex (36-28 Ma), which was the major sediment source
- The exhumation of the Rhodope Complex and the formation of the Thrace Basin involved crustal rotation and possibly crustal flow

Author Contributions:

Conceptualization: Aral I. Okay, Ercan Özcan
Data curation: Muzaffer Siyako
Formal analysis: Ercan Özcan, Muzaffer Siyako, Kerem A. Bürkan, Michael D. Bidgood, David Shaw, Michael D. Simmons
Funding acquisition: Aral I. Okay

Thrace Basin—An Oligocene Clastic Basin Formed During the Exhumation of the Rhodope Complex

Aral I. Okay[1,2] , Ercan Özcan[2,†], Muzaffer Siyako[3], Kerem A. Bürkan[3], Andrew R. C. Kylander-Clark[4] , Michael D. Bidgood[5], David Shaw[6], and Michael D. Simmons[7]

[1]Eurasia Institute of Earth Sciences, Istanbul Technical University, İstanbul, Turkey, [2]Department of Geological Engineering, Faculty of Mines, Istanbul Technical University, İstanbul, Turkey, [3]Exploration Department, Türkiye Petrolleri A.O., Ankara, Turkey, [4]Department of Earth Sciences, University of California, Santa Barbara, Santa Barbara, CA, USA, [5]GSS (Geoscience) Ltd, Oldmeldrum, UK, [6]Biostratigraphic Associates (UK) Ltd, Stoke-on-Trent, UK, [7]Halliburton, Abingdon, UK

Abstract Some orogenic sedimentary basins are difficult to assign to a particular category. An example is the hydrocarbon-bearing Thrace Basin in the northern Aegean. It has more than 9-km-thick Cenozoic clastic sediment, and is spatially associated with the Rhodope metamorphic core complex in the west, and with the Tethyan subduction-accretion complexes in the south, and is cut by the North Anatolian Fault and its precursors. It has been interpreted variously as an intramontane, a forearc, or an orogenic collapse basin. Here, we provide new geochronological and biostratigraphic data to constrain the tectonic evolution of the Thrace Basin. The new data indicate that as an individual depocenter the Thrace Basin has a short age span (late Eocene—Oligocene, 36–28 Ma) and more than 90% of the basin fill consists of early Oligocene (34–28 Ma) siliciclastic turbidites, deposited at rates of 1.0 km/my. Paleocurrents and new detrital zircon U-Pb ages show that the Rhodope Complex was the main sediment source. The exhumation of the northern Rhodope Complex (36–28 Ma) was coeval with the main subsidence in the Thrace Basin (34–28 Ma), and involved clockwise crustal rotation in the northern Aegean and possibly crustal flow from underneath the Thrace Basin. Crustal rotation is indicated by the paleomagnetic data, regional stretching lineations in the Rhodope Complex, and the triangular shape of the Thrace Basin. The rotating crustal block must have been bounded in the south by a sinistral fault zone; the location of which corresponds largely with the present day North Anatolian Fault.

1. Introduction

Basins are regions on Earth's crust with thick sedimentary accumulations and are important as centers for hydrocarbon accumulations and sequestration of anthropogenic CO_2. They form in various tectonic settings and come in widely differing shapes, sizes, and ages (e.g., Allen & Allen, 2013; Evenick, 2021; Ingersoll, 2011). Most basins can be related to a particular tectonic setting and attributed to a basin type. However, the origin of some basins is controversial. An example is the Cenozoic Thrace Basin in southwestern Balkans (Figure 1), which is described in various studies as an intramontane (Doust & Arıkan, 1974; Perinçek, 1991), a forearc (Görür & Okay, 1996; Maravelis et al., 2016; Saner, 1980), an orogenic collapse (Cavazza et al., 2013), a detachment basin (e.g., Kilias et al., 2013) or an upper-plate extensional basin related to slab retreat in front of the Pindos remnant ocean (d'Atri et al., 2012). Part of the reason for the controversy is a lack of precise data on the age of the basin infill. Most of the Thrace Basin is covered by Miocene and younger sediments (Figure 2), and there are only a few sections where the sedimentary sequence can be studied in outcrop. Furthermore, most of the stratigraphic sequence consists of siliciclastic turbidites, which have poor biostratigraphic resolution. On the other hand, as the Thrace Basin produces gas and oil, there are a large number of seismic lines and wells, which provide information on the basin lithostratigraphy and geometry (e.g., Doust & Arıkan, 1974; Turgut et al., 1991). Here we provide new geochronological and biostratigraphic age data from outcrop and subsurface to constrain the timing of major subsidence in the Thrace Basin and investigate the relation between subsidence of the Thrace Basin and tectonics in the Balkans and Aegean. These new data show that the bulk of subsidence in the Thrace Basin occurred not during the Eocene, as generally assumed, but in the early Oligocene (34–28 Ma) and was coeval with the exhumation of the Rhodope Complex. New detrital zircon ages from the Oligocene sandstones, and published paleocurrent and petrographic data (Caracciolo et al., 2015; Cavazza et al., 2013; d'Atri et al., 2012) also indicate the Rhodope Complex as the major sediment source.

Investigation: Aral I. Okay, Ercan Özcan, Muzaffer Siyako, Kerem A. Bürkan, Michael D. Bidgood, David Shaw, Michael D. Simmons
Methodology: Aral I. Okay, Michael D. Simmons
Supervision: Michael D. Bidgood, David Shaw, Michael D. Simmons
Validation: Muzaffer Siyako, Kerem A. Bürkan, Michael D. Simmons
Writing – original draft: Aral I. Okay

2. Geological Setting of the Thrace Basin

The Thrace Basin is a large hydrocarbon bearing Cenozoic clastic basin in the southeastern Balkans (Figure 1, Kopp et al., 1969; Siyako & Huvaz, 2007; Turgut et al., 1991). It is roughly triangular in shape with its sides approx. 200 km in length and a surface area of about 25,000 km^2. Most of the Thrace Basin lies in Turkey with its margins extending into Greece and Bulgaria. The sedimentary sequence in the center of the Thrace Basin exceeds nine km in thickness (Figure 1).

The Thrace Basin is located at the junction of three paleotectonic units: the Sakarya Zone, the Strandja Massif and the Rhodope Complex (Figure 1b). Magnetotelluric studies and gravity modeling indicate that the crustal thickness changes from 40 to 44 km under the Strandja Massif to 28–32 km or less under the Thrace Basin (M. Bayrak et al., 2004; İlkışık, 1981; Kende et al., 2017). The present crustal thickness is estimated to be 50 km thick under the Rhodope Complex (c.f. Burg, 2012).

The Strandja Massif separates the Thrace Basin from the Black Sea, which is a Late Cretaceous backarc basin with more than 14 km of Upper Cretaceous to Recent sediments (e.g., Nikishin et al., 2015; Robinson et al., 1996). The Strandja Massif consists of metamorphic and granitic rocks; it underwent metamorphism and penetrative deformation during the latest Jurassic and the metamorphic rocks are unconformably overlain by Upper Cretaceous marine sediments along the Black Sea coast (e.g., Okay et al., 2001; Sağlam et al., 2023; Sunal et al., 2011). The apatite fission track (AFT) central ages from the Strandja Massif are Late Cretaceous (Cattò et al., 2018). During the Cenozoic the Strandja Massif formed a broad subaerial arch separating the Thrace Basin from the Black Sea (e.g., Okay et al., 2019). The Rhodope Complex is also made up of metamorphic and granitic rocks but, in contrast to the Strandja Massif, it has a much younger thermal history. The Ar-Ar and AFT ages from the Rhodope Complex are Cenozoic (e.g., Kounov et al., 2015, 2020; Lips et al., 2000; Márton et al., 2010). The contact between the Rhodope Complex and the Strandja Massif is constituted by the poorly defined Maritza Fault largely covered by Cenozoic sediments (Figure 1). East of the Rhodope Complex there are low-grade metamorphic rocks ascribed to the Circum-Rhodope Complex (Figure 1a, e.g., Bonev & Stampfli, 2003; Kauffmann et al., 1976). Eocene-Oligocene sedimentary rocks of the Thrace Basin lie unconformably over these low-grade metamorphic rocks in Greece, Bulgaria, and Turkey (e.g., Boyanov & Goranov, 2001; Kopp, 1965; Okay et al., 2010).

The Sea of Marmara forms part of the present southern boundary of the Thrace Basin. It formed during the last 5 million years through the action of the North Anatolian Fault (e.g., Armijo et al., 1999; Okay et al., 2000) and is, thus, younger than the Thrace Basin. It cuts the Thrace Basin in the south, and the onland segment of the North Anatolian Fault in this region is called the Ganos Fault (Figure 1).

During the late Eocene and Oligocene, the Sakarya Zone south of the Marmara Sea was largely an erosional area (Okay et al., 2020). The only Upper Eocene—Oligocene outcrops are found in the Biga peninsula (Figures 1 and 2, E. Özcan et al., 2018). The Sakarya and Istanbul zones are separated by the Intra-Pontide suture (e.g., Akbayram et al., 2013). Small outcrops of serpentinite and Late Cretaceous blueschists (ca. 85 Ma) along the North Anatolian Fault in southern Thrace are considered to represent fragments of this Intra-Pontide ocean (Figure 2, Okay et al., 2010; Topuz et al., 2008). Eocene-Oligocene sequences of the Thrace Basin also extend to the northern Aegean islands of Imroz and Limnos, which are displaced westwards by about 88 km along the North Anatolian Fault (Figure 1, Akbayram et al., 2016).

2.1. Stratigraphy and Development of the Thrace Basin

The Thrace region contains three sedimentary packages separated by unconformities corresponding to periods of deformation and uplift. These are: (a) Lower Eocene, (b) middle/upper Eocene—Oligocene, and (c) Miocene-Pliocene (Figure 3). Of these three sequences, the lower Eocene and Miocene-Pliocene ones are also found over wide areas in northwest Turkey (Figures 1 and 2) and are not specific for the Thrace Basin. On the other hand, the middle/upper Eocene—Oligocene sequence is confined to the Thrace Basin; during this period most of northwest Anatolia was an erosional area (Okay et al., 2020). Therefore, the Thrace Basin as a separate, distinct sedimentary basin existed only during the late middle Eocene and Oligocene.

2.1.1. Lower Eocene Clastic Rocks—Erosional Remnants of an Earlier Depositional Cycle

Seismic sections tied to oil wells show that the central part of the Thrace Basin is underlain by lower Eocene clastic rocks, ascribed to the Hamitabat Formation (Figure 2, Bürkan, 1992a; Siyako, 2006b; Siyako & Huvaz, 2007). Information on the Hamitabat Formation is based largely on well logs and is limited; it apparently encompasses
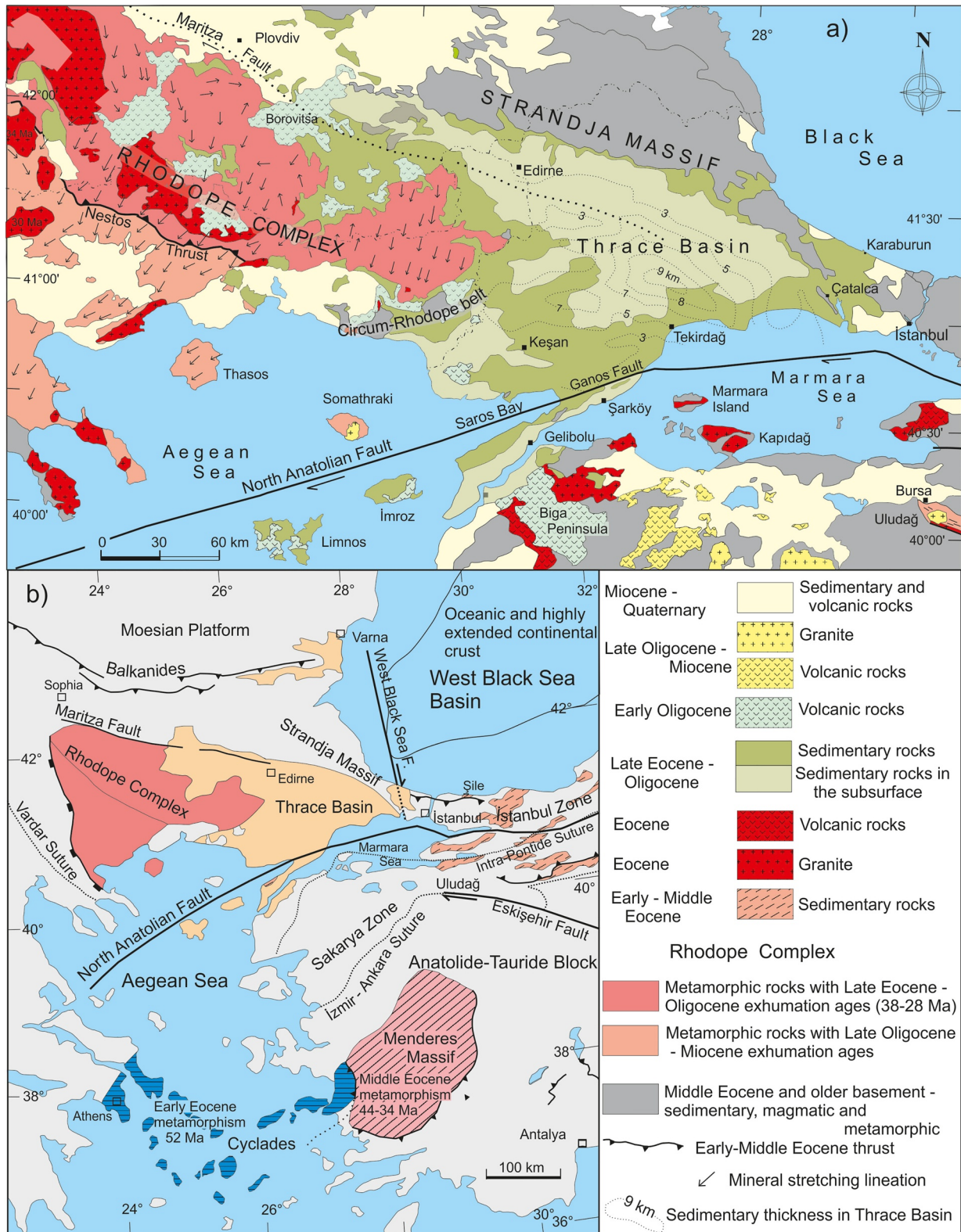
Figure 1. (a). Geological map of the Rhodope Complex and the Thrace Basin. The sedimentary thickness isopachs in the Thrace Basin are modified from Turgut et al. (1991) and Siyako and Huvaz (2007). The stretching lineations are from Burg (2012) and Brun and Sokoutis (2007). (b). Thrace Basin and Rhodope Complex in a wider Aegean tectonic setting.
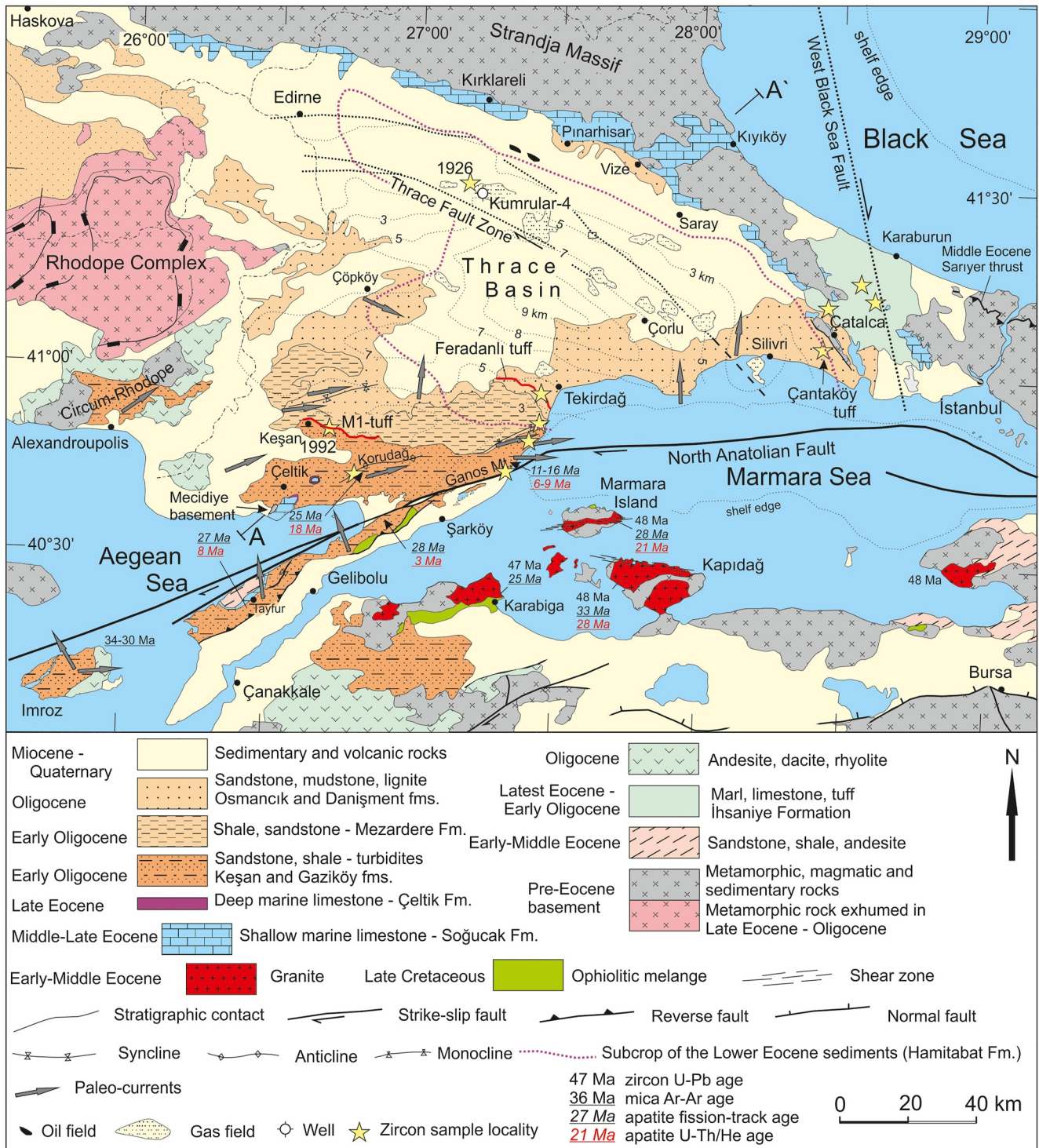
Figure 2. Geological map of the Thrace Basin and northwest Anatolia. The numerical ages are from Ustaömer et al. (2009), Altunkaynak et al. (2012), Okay et al. (2022), Zattin et al. (2010), and Hejl et al. (2010). The paleo-current data are from Şenol (1980), d'Atri et al. (2012), and Cavazza et al. (2013). The map is compiled from Turgut et al. (1991) and Türkecan and Yurtsever (2002). The outlines of the subsurface lower Eocene Hamitabat Formation are from Bürkan (1992a).

a variety of facies from turbidites to continental clastic rocks, and locally reaches a thickness of more than 2 km (Gürgey, 2009; Siyako & Huvaz, 2007; Turgut et al., 1991). In seismic sections the top of the Hamitabat Formation is a marked by an unconformity (c f. Figure 8 of Siyako and Huvaz (2007)). Vitrinite reflectance values also exhibit a sudden decrease above the Hamitabat Formation (Huvaz et al., 2005). These observations indicate a
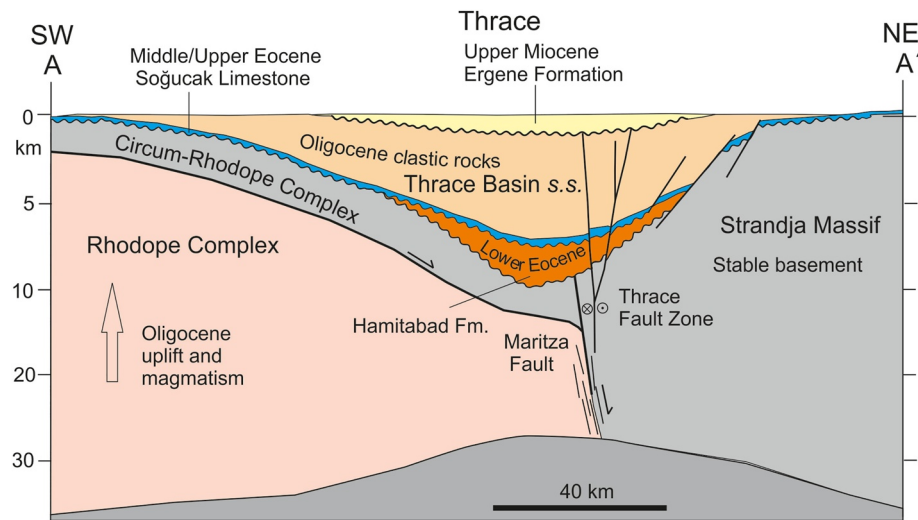
Figure 3. Schematic cross-section across the Thrace showing its three depositional systems of early middle Eocene, late Eocene-middle Oligocene, and late Miocene ages. In the deepest part of the basin the total thicknesses pertaining to these periods are approximately 3, 5, and 1 km, respectively (Perinçek et al., 2015; Turgut et al., 1991). The Thrace Basin *s.s.* comprises Soğucak limestones and the Oligocene clastic rocks. For location of the section see Figure 2.
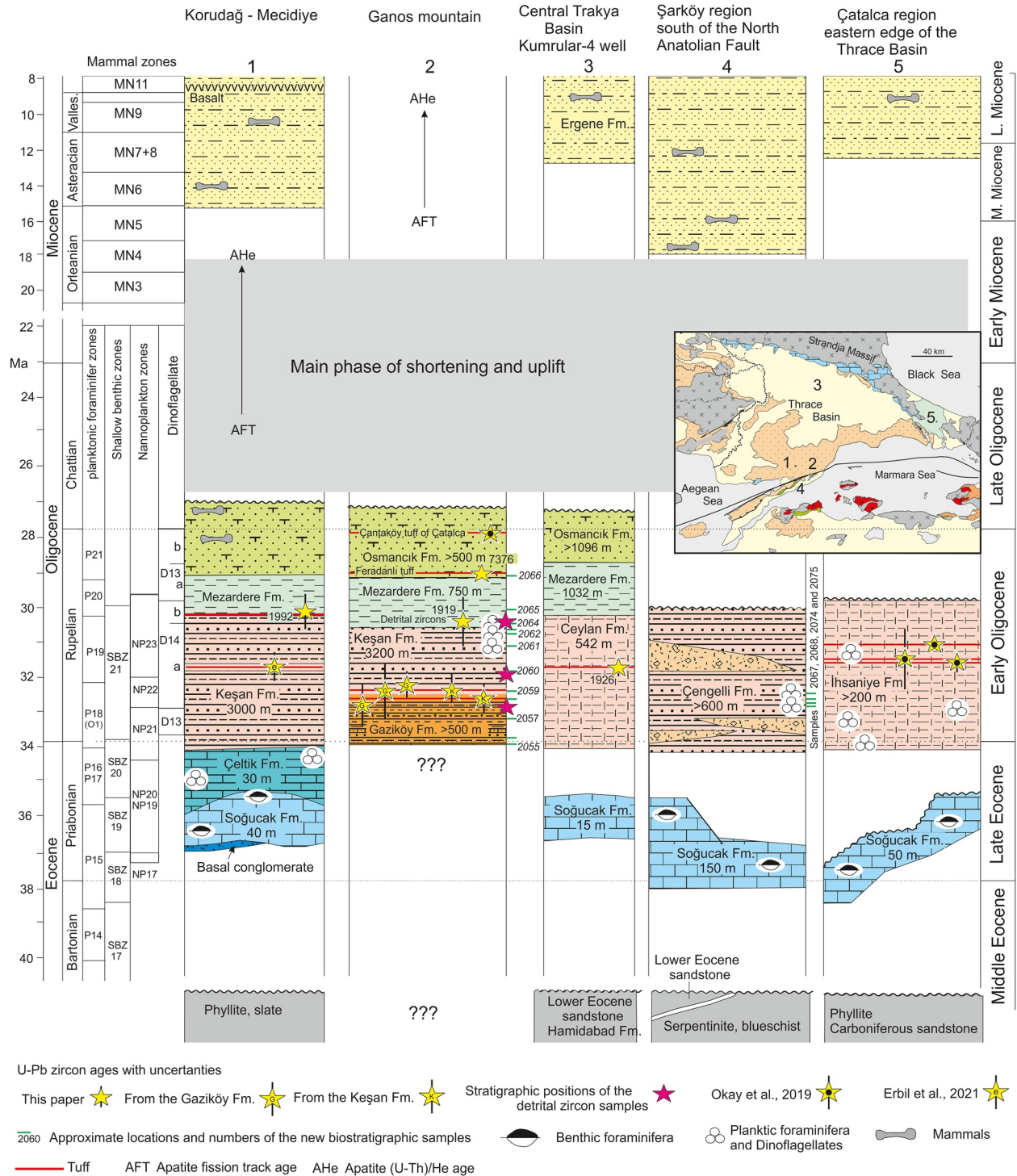
major break in sedimentation in the middle Eocene, which was a time of contractional deformation, uplift, and erosion in Anatolia and in the Balkanides (e.g., Z. Özcan et al., 2012; Sinclair et al., 1997).

In contrast to its wide subsurface distribution, there are only two small outcrops of the lower Eocene rocks in the Thrace Basin. A lower Eocene sequence crops out on the northern margin of the Gelibolu peninsula (Figure 2). It consists of siliciclastic turbidites, 750-m in thickness, overlain by fluviatile red beds (Önal, 1986). The lower Eocene series on the Gelibolu peninsula are unconformably overlain by the late middle Eocene (early Bartonian) shallow marine limestones (E. Özcan et al., 2010). The second lower Eocene locality is located northeast of Şarköy, where a 30-m thick sequence of sandstone, calcareous sandstone and shale is dated to early Eocene. It is also unconformably overlain by the late middle to upper Eocene limestones (Figure 4, E. Özcan et al., 2010).

Most studies consider the lower Eocene succession, including the Hamitabat Formation, as part of the Thrace Basin (e.g., Elmas, 2012; Siyako & Huvaz, 2007; Turgut et al., 1991). However, lower Eocene successions, similar to the Hamitabat Formation, are widespread in northwestern Turkey (Figures 1b and 2, E. Özcan et al., 2020; Z. Özcan et al., 2012). Early Eocene sedimentation occurred over a large area in Anatolia and the Balkans, and the Thrace Basin did not exist as a separate depocenter during the early Eocene (Figure 5a). The lower Eocene sedimentary rocks were partly eroded during the middle Eocene shortening and uplift. The Hamitabat Formation in the Thrace Basin represents an erosional remnant from the early Eocene depositional cycle.

2.1.2. Middle Eocene Deformation and Uplift

In northwest Anatolia, Eocene sedimentation and associated volcanism lasted until the early middle Eocene (Lutetian) (Okay et al., 2020; E. Özcan et al., 2020; Z. Özcan et al., 2012); this was followed by contractional deformation and uplift (Figure 5b). The middle Eocene constitutes one of the main Alpine orogenic phases in Anatolia. The Paleozoic sequence of the Istanbul region was thrust north over Upper Cretaceous volcanic rocks (Figure 2, A. F. Baykal, 1943; A. F. Baykal & Önalan, 1980). This thrust can be traced for over 50 km on both sides of the Bosphorus (Figure 2) and is recorded as an intra-Eocene angular unconformity in the Şile region on the Black Sea coast (A. F. Baykal & Önalan, 1980; E. Özcan et al., 2007). The north-vergent thrusting in the Balkanides also started in the middle Eocene (Sinclair et al., 1997) and was widespread in the southern Balkans (Burchfiel et al., 2008). South-vergent Eocene thrusts close to the İzmir-Ankara suture in west-central Anatolia created a middle Eocene foreland basin (Mueller et al., 2019). The Menderes Massif was buried under the southwestward moving Lycian nappes and was metamorphosed during the middle Eocene (43–35 Ma, e.g., Schmidt et al., 2015). The widespread middle Eocene contraction and resultant uplift was followed by erosion over large areas. The marine sedimentation in northwest Anatolia, as opposed to Thrace, ended in the early Lutetian (ca. 45 Ma) and the region has been a land area since then (Figures 5b–5d, Okay et al., 2020).

Figure 4. Stratigraphic sections of the Thrace Basin with new and published tuff ages and biostratigraphic data. The stratigraphy is from Siyako (2006b), Erbil et al. (2021), and Okay et al. (2010, 2019) modified to the new age data. The biostratigraphic zonation is after Speijer et al. (2020) and Steininger and Wessely (2000). The Miocene mammal ages are from Ünay & De Bruijin (1984) and Geraads et al. (2005). The inset shows the locations of the stratigraphic sections. The approximate locations of the biostratigraphic samples that have yielded results, are shown by paleontological symbols.

2.1.3. Late Middle Eocene—Oligocene Sequence—The Thrace Basin *Stricto Sensu*

The sedimentary sequence in the Thrace Basin *s.s.* starts with middle to upper Eocene shallow marine limestones, the Soğucak Formation, which are only found in the Thrace region and in the Biga peninsula (Figure 5c). The
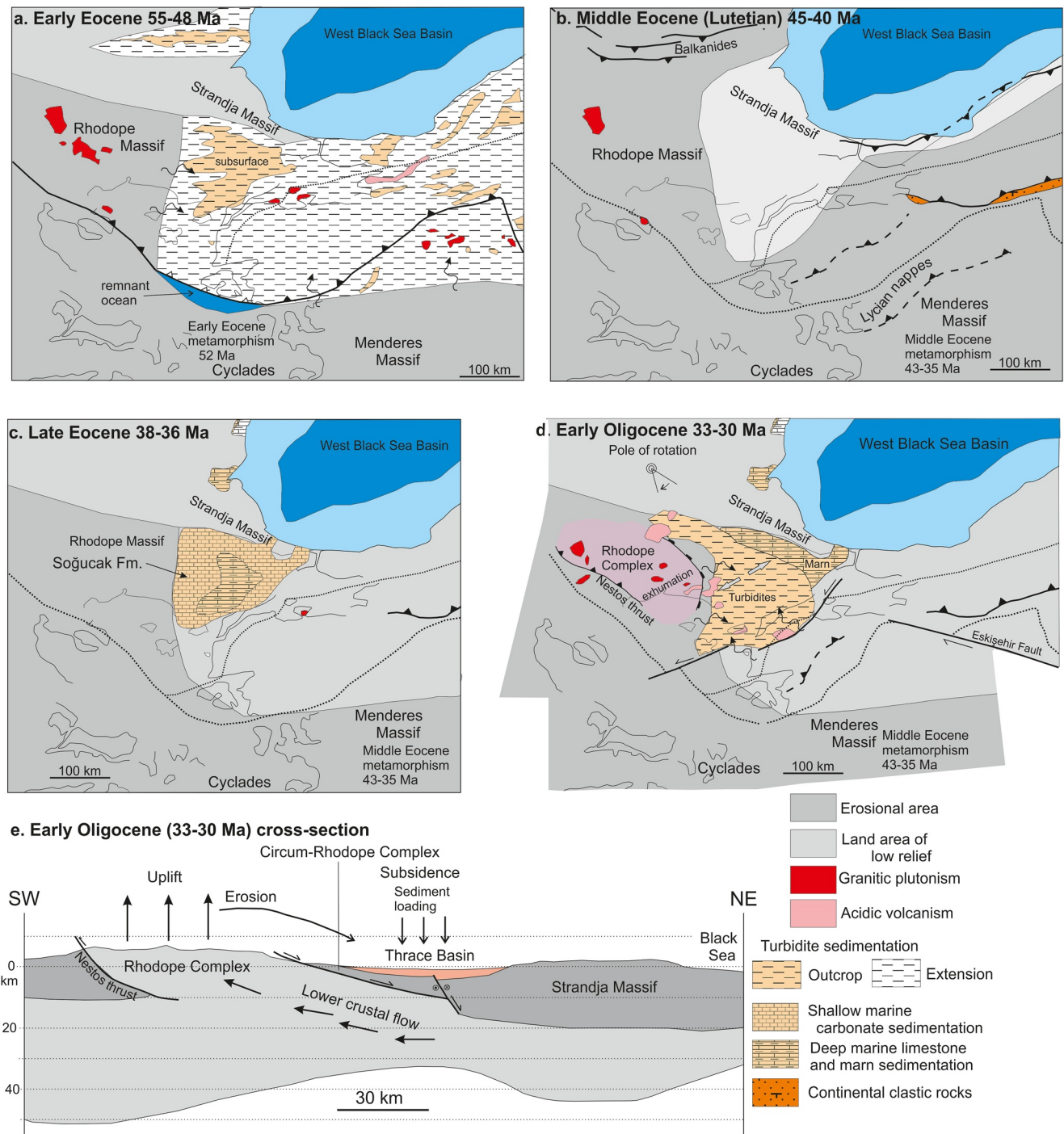
Figure 5. Paleogeographic maps of the northern Aegean for the Eocene and Oligocene (a–d) and a conceptual model for the exhumation of the Rhodope Complex and the formation of the Thrace Basin.

rest of northwest Anatolia was an erosional area during this period (Okay et al., 2020). The Eocene Soğucak Formation is overlain by a thick clastic series; locally there is a thin sequence of upper Eocene pelagic limestones between the Soğucak Formation and the overlying turbidites. The clastic sequence crops out best at Ganos Mountain (Figure 2, Okay et al., 2004); it starts with distal turbidites, which pass up into medial turbidites, deltaic shales and eventually into paralic sandstones. Our new geochronological and biostratigraphic results come from this part of the Thrace basin, the stratigraphy of which will be described in detail with new results in a subsequent section.

2.1.4. Late Oligocene—Middle Miocene Shortening and Late Miocene Sedimentation

Sedimentation in the Thrace Basin terminated in the middle Oligocene through contractional deformation and uplift. The age of the deformation is constrained by the latest early Oligocene top age of the underlying Oligocene sequence (ca. 28 Ma) and the unconformably overlying poorly consolidated upper Miocene fluviatile sand and clay of the Ergene Formation (Erbil et al., 2021). The Ergene Formation covers a wide area in Thrace and reaches a thickness of over 1,000 m (Figure 2, Perinçek et al., 2015). It contains late Miocene (MN10, 10–9 Ma) vertebrate fossils (Geraads et al., 2005) and is intercalated with late Miocene alkali basaltic lava flows dated 11.7–8.6 Ma (Figure 4, Kaymakci et al., 2007). The AFT and apatite U-Th/He data from the Eocene sandstones narrows down the time of the deformation to the latest Oligocene to early Miocene (25–18 Ma, Figure 2, Zattin et al., 2010).

The late Oligocene—early Miocene shortening led to the formation of long wave-length folds, such as the Korudağ anticline, and other large-scale folds north of Keşan (Figure 2, Erbil et al., 2021; Okay et al., 2004). The orientation of the fold axis indicates NNW-SSE shortening. A major dextral fault zone, the Thrace Fault, was also initiated in this period (Figure 2, Perinçek, 1991). The Thrace Fault zone follows the trace of the Maritza Fault and is overlain by undeformed upper Miocene sands (Perinçek, 1991; Perinçek et al., 2015). Contraction during the late Oligocene-middle Miocene was also widespread in the southern Balkans (e.g., Burchfiel et al., 2008) and forms an interlude between two extensional periods of late Eocene—middle Oligocene and late Miocene—Recent, respectively (Erbil et al., 2021; Georgiev et al., 2010).

3. Methods

During the present study, samples were collected for biostratigraphy and geochronology. For biostratigraphy 12 samples were collected from the well-exposed Ganos section and four samples from south of the Ganos Fault (Figure 4). The samples were processed for foraminifera and palynomorphs (especially dinoflagellates). Eleven samples were studied for zircon U-Pb geochronology from the Ganos and Korudağ mountains, and one sample from one of the deep wells in the center of the Thrace Basin (Figures 2 and 4); they comprise nine tuff samples for magmatic ages and three sandstone samples for detrital zircons ages.

3.1. Paleontological Methods

The samples were prepared for foraminiferal analysis using the standard methodology described in Armstrong and Brasier (2005). To summarize, dissolution in a 10% solution of hydrogen peroxide was undertaken, and the residues dried and then concentrated using a nest of sieves. Foraminifera (and ostracoda and other miscellaneous microfossils) were then transferred to slides for examination with a binocular microscope.

Samples were prepared for palynological analysis using the standard methods described by Armstrong and Brasier (2005). Approximately 30 g of cleaned and crushed sample was used for processing. Standard HCl (20%) and HF (40%) chemical treatments were sequentially used to dissolve the carbonate and silicate content of the samples. Multiple resieving over 10-μm mesh cloth, including rewarming in 20% HCl to remove silico-fluoride precipitates, was performed. The sample was then assessed to establish further processing requirements (oxidation) to concentrate the palynomorphs present (a split of the unoxidized kerogen was taken at this time). Oxidation involved cold bathing in concentrated nitric acid (70%) for between 2 and 5 min, followed by further sieving and neutralization with water. Further microscopic examination determined the amount of ultrasonic treatment (between 5 and 15 s), which helped to concentrate the palynomorphs further. Both unoxidized and oxidized kerogen residues were separately mounted onto a labeled glass slide and permanently glued using Norland optical adhesive No. 63. The paleontological results and the UTM coordinates of the samples are given in Table S1.

3.2. Mineral Separation, Preparation, and Laser Ablation ICPMS Zircon Dating

Zircon fractions from tuff and sandstone samples were separated at the Istanbul Technical University using standard mineral separation procedures. This included crushing whole rock samples to sand-size grains, sieving, repeated rinsing, and cleaning of samples in water and acetone and passing the samples through a Frantz magnetic separator. For zircon separation we used heavy liquids followed by handpicking under a stereoscopic microscope. The zircons were mounted in epoxy and were polished at Istanbul Technical University. Cathodoluminescence

(CL) images of the polished zircons were captured on a Zeiss Evo 50 EP scanning electron microscope at Hacettepe University in Ankara. The CL images of the analyzed zircons are given in Figure S1 in Supporting Information S1. The zircon U-Pb analysis were made using laser-ablation inductively coupled plasma mass spectrometry at the University of California, Santa Barbara (Kylander-Clark et al., 2013). The analyses were performed using a Photon Machines Excite 193 nm Excimer laser coupled to a Nu Plasma HR, using a spot size of 20 µm and a rep rate of 4 Hz for 15 s. The primary reference material was 91,500, and secondary RMs included GJ1 (Horstwood et al., 2016), Temora2 (Black et al., 2004), Plesovice (Sláma et al., 2008), and 94–35 (Klepeis et al., 1998); all reference materials yielded ages within 1% of their accepted values. Long-term reproducibility in secondary reference materials is <2%, and, as such, should be used when comparing ages obtained within this analytical session to ages elsewhere. We report dates >1,400 Ma as ^{207}Pb/^{206}Pb ages, and dates <1,400 Ma as 207-corrected ^{206}Pb/^{238}U ages, and only consider dates that are within 10% of concordia. The zircon U-Pb ages are summarized in Table 1. Sample descriptions and UTM coordinates of the analyzed samples are given in Table S2 in Supporting Information S2, and the analytical data in Tables S3–S14 in Supporting Information S2.

4. Stratigraphy of the Thrace Basin *s.s.* in the Light of the New Geochronologic and Biostratigraphic Data

The Thrace Basin *s.s.* starts with widespread but thin shallow marine limestone sequence, which is overlain by a thick regressive clastic sequence ranging from distal turbidites to paralic sandstones. This clastic sequence can best be studied in outcrop in the Ganos Mountain, which was uplifted through the action of the North Anatolian Fault (Figure 2, Okay et al., 2004). The Ganos Mountain exposes a 5-km thick regressive clastic series starting with distal turbidites, which pass up into medial turbidites, deltaic shales, and paralic sandstones. The Korudağ region northwest of the Ganos Mountain also provides a good section of the medial turbidites (Figure 2). Both the Ganos and Korudağ sections were studied and sampled during this study.

4.1. The Soğucak Formation—Eocene Shallow Marine Limestones Marking the Base of the Thrace Basin

Shallow marine middle to upper Eocene limestones, locally with a basal horizon of continental sandstone and conglomerate, lie at the base of the Thrace Basin *s.s.* This Soğucak Formation is usually less than 50 m thick but forms a prominent and ubiquitous basal unit (Figure 3). In the northeast it lies unconformably over the metamorphic rocks of the Strandja Massif (Figure 2, Less et al., 2011); the present contacts between the Eocene limestones and the Strandja Massif largely corresponds to the middle/late Eocene shoreline. In the west the Soğucak Formation lies unconformably over the metamorphic rocks of the Circum-Rhodope Complex (e.g., Boyanov & Goranov, 2001; Kopp, 1965; Okay et al., 2010). South of the Ganos Fault coeval limestones lie unconformably over serpentinite and pelagic sedimentary rocks. Locally, the top of the Soğucak Formation is marked by an unconformity (Okay et al., 2019).

In previous studies, the age of the Soğucak Formation is constrained by shallow benthic foraminifera, and is highly diachronous (Figure 4). The earliest ages from the Soğucak Formation are found on the island of Imroz, where it is dated as early Bartonian (SBZ15-17, ca. 41 Ma, E. Özcan et al., 2010). In the rest of the Thrace Basin the age of the Soğucak Formation is late Bartonian to Priabonian (SBZ18-20, 38–34 Ma, Less et al., 2011; Yücel et al., 2020). The age of the Soğucak Formation varies widely over short distances indicating that the sea transgressed over an uneven topography.

4.2. The Çeltik Formation—Abrupt Subsidence at the End of the Eocene

In the western part of the Thrace Basin, west of Korudağ, the shallow marine carbonates of the Soğucak Formation are sharply overlain by a thin sequence of upper Eocene pelagic limestone, calciturbidite and marl (Figures 2 and 4). Erbil et al. (2021) report a rich planktic foraminifera fauna of latest Eocene age (P16-17, 35–34 Ma) from this Çeltik Formation, which is only 30-m thick. The fauna and lithology mark a change from shallow marine to deep marine deposition. The Çeltik Formation is absent in many outcrops possibly due to local erosion by later turbidity currents.

4.3. Lower Oligocene Turbidites—The Gaziköy, Keşan, and Ceylan Formations

The Eocene limestones in the Thrace Basin are succeeded by a turbidite sequence, which forms a regressive series up to 5 km thick (e.g., Aksoy, 1987; Doust & Arıkan, 1974; Şen & Yıllar, 2016; Siyako, 2006b; Siyako

Table 1
New and Published U-Pb Zircon Ages From the Thrace Basin

U-Pb age (Ma)	Number of zircon ages used for concordia	Stratigraphic age	Locality	Sample no.	Source
From the tuffs					
Gaziköy formation					
32.5 ± 0.5	15	Early Oligocene	Ganos Mountain	2139	This study
32.4 ± 0.7	13	Early Oligocene	Ganos Mountain	2140	This study
31.6 ± 1.5	17	Early Oligocene	Ganos Mountain	2143	This study
32.0 ± 0.6	2	Early Oligocene	Ganos Mountain	12319	This study
Keşan formation					
32.6 ± 0.4	12	Early Oligocene	Ganos Mountain	2145	This study
32.5 ± 0.4	18	Early Oligocene	Ganos Mountain	2149	This study
31.7 ± 0.4	19	Early Oligocene	Korudağ	1933	Erbil et al. (2021)
30.4 ± 0.8	4	Early Oligocene	Korudağ	1992	This study
Ceylan formation					
31.6 ± 0.5	20	Early Oligocene	Kumrular-4 well	1926	This study
Osmancık formation					
28.9 ± 0.1	34	Early Oligocene	Feradanlı tuff, Ganos Mountain	7376	This study
27.9 ± 0.2	41	Latest Early Oligocene	Çantaköy tuff, Çatalca	1456	Okay et al. (2019)

Formation	Total number of ages	Concordant ages and youngest age (Ma)	Locality	Sample no.	
Detrital zircon U-Pb data from the lower Oligocene sandstones					
Gaziköy	23	22–77	Ganos Mountain	1915	This study
Keşan	49	48–43	Ganos Mountain	1917	This study
Mezardere	105	100–30	Ganos Mountain	1919	This study

& Huvaz, 2007). It is best observed in outcrop at Ganos Mountain on the northern shores of the Marmara Sea (Figures 6, 7, and 8a). The Ganos section starts with distal turbidites, more than 855 m thick, of black siltstones intercalated with dark shales and with rare tuff beds (Figures 6, 8b, and 8c).

Tuff layers form a volumetrically small (<1% of the sequence) part of the Thrace Basin but provide dateable chronological markers. In the present study nine tuff beds were dated using zircon U-Pb method (Table 1). The tuffs form white, pale gray, fine to medium grained, commonly bedded or laminated horizons with thicknesses ranging from a few tens of centimeters to over 20 m (Figure 9d). They are commonly intercalated with sandstone and shale. Petrographically the tuffs are generally fine to very fine grained and consist of volcanic glass, feldspar, quartz, volcanic lithics, and occasionally biotite clasts. Zircons from the tuffs are commonly prismatic to acicular and show igneous oscillatory zoning (Figure S1 in Supporting Information S1).

In all previous studies this Gaziköy Formation was considered of early to middle Eocene age (e.g., Aksoy, 1987; Doust & Arıkan, 1974; Elmas, 2012; Görür & Okay, 1996; Okay et al., 2004; Siyako, 2006b; Siyako & Huvaz, 2007; Sümengen & Terlemez, 1991; Turgut et al., 1991; Yıldız et al., 1997). Elmas et al. (2016) also published an early Eocene zircon U-Pb age of 51.0 ± 2.1 Ma from a tuff bed in the Gaziköy Formation. To confirm this age, we dated zircons from a tuff bed in the Gaziköy Formation (sample 12319). The pale gray tuff bed is 20 m thick and occurs above black shales and siltstones (Figure 9b). Thirty-one zircon grains were dated, only nine were concordant, and two concordant zircon grains gave an early Oligocene age of 31.6 ± 0.4 Ma (Figure 9a, Table S11 in Supporting Information S2). To test this unexpectedly young age, we dated zircons from three other tuff beds (samples 2139, 2140 and 2143) from the Gaziköy Formation (Figure 6). All of the 45 zircon ages from three tuffs beds were concordant and all yielded early Oligocene ages of 32.8 ± 0.3, 32.4 ± 0.7, and 32.2 ± 0.4 Ma, respectively (Figure 9, Tables S5–S7 in Supporting Information S2). The zircon ages show conclusively that the Gaziköy Formation is not early Eocene but early Oligocene in age. The early Eocene zircon ages reported by Elmas et al. (2016) from the Gaziköy Formation must be from xenocrysts, especially since Elmas et al. (2016) also mention the presence of "anomalously younger ages" in their data set. We also analyzed four shale samples (2055–2058) from the Gaziköy Formation for foraminifera and palynology, however, no age diagnostic fossils were recovered.

The distal turbidites pass up into medial to proximal turbidites of the Keşan Formation, which has a thickness of 3.2 km (Figures 4, 6, 8a, and 8c, Okay et al., 2004). Tuff beds are also present in the lower levels of the Keşan Formation (Figure 10b). Two tuff layers (samples 2145 and 2149) in the Keşan Formation were dated (Figure 6). Thirty concordant zircons from both samples also yielded early Oligocene ages of 32.6 ± 0.4 and 32.4 ± 0.3 Ma, respectively, indistinguishable from those from the top of the Gaziköy Formation (Figures 10a and 10c, Tables S8 and S9 in Supporting Information S2). We also collected several samples (2059–2063) from the shales of the Keşan Formation for paleontological study. Most samples had poor recovery, or contained extensively reworked fossils (Table S1). Nonetheless, sample 2062 from close to the top of the Keşan Formation (Figure 6) contained dinoflagellates (*Wetzeliella gochtii*, *Wetzeliella simplex*) indicative of early Oligocene biozone D14a sensu Costa and Manum (1988). Biozone D14a has an approximate age range of 33.2–30.2 Ma according to Speijer et al. (2020). The biostratigraphically calibrated ages from sample 2062 overlap with the U-Pb zircon age from the tuffs and supports an early Oligocene age for the Keşan Formation. An underlying sample, 2061, yielded the dinoflagellates *Enneadocysta pectiniformis*, *Cordosphaeridium cantharellus*, and *Reticulatosphaera actinocoronata* indicating a general late Eocene—early Oligocene age range.

The Keşan Formation also crops out widely in the Korudağ region north of the Saros Bay (Figure 2), where it also includes several white tuff horizons. Erbil et al. (2021) published an early Oligocene zircon U-Pb age of 31.7 ± 0.4 Ma from a tuff bed in the Keşan Formation in Korudağ.

Distal turbidites with tuff beds also crop out on the Gelibolu peninsula, where they lie on the shallow marine limestones of the Soğucak Formation (Figure 2, Önal, 1986). D'Atri et al. (2012) report an Ar-Ar biotite and feldspar age of 30.2 ± 0.2 Ma from a tuff bed from the Gelibolu peninsula. The new data indicate that the turbidites above the Soğucak Formation (Gaziköy and Keşan formations) were deposited over a short interval in the early Oligocene (34–30 Ma, Figure 4).

The center of the Thrace Basin constitutes the locus of sediment accumulation and also the area of most natural gas production (Figure 2). It forms a low-lying plain with a cover of continental Miocene sands. Information on the nature of the stratigraphic sequence and its thickness comes entirely from wells and seismic sections
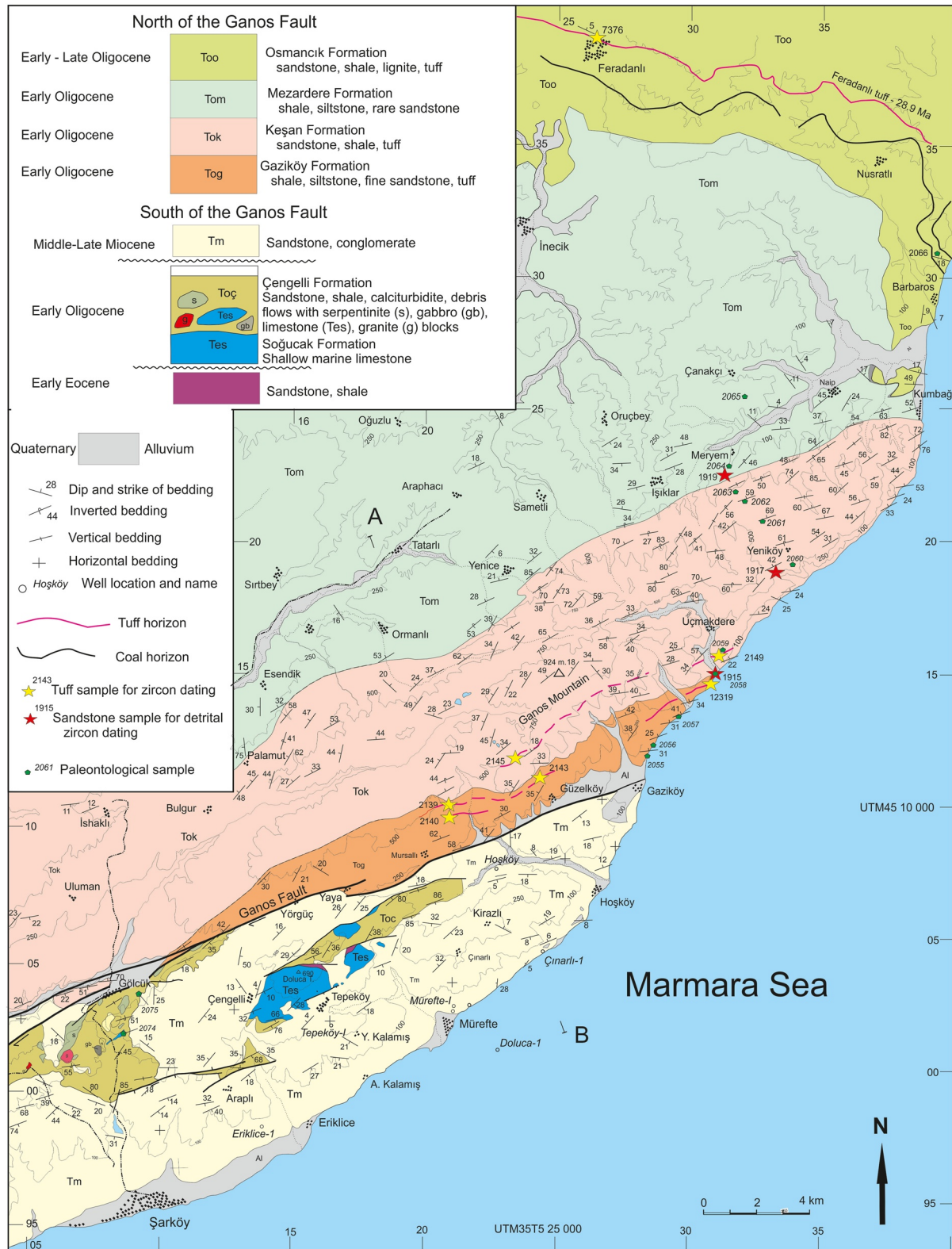
Figure 6. Geological map of the Ganos Mountain and Şarköy region in southern Thrace (based Okay et al. (2004, 2010)). The traces of the Feradanlı tuff and the lignite horizon are from Lebküchner (1974). For location see Figure 2.
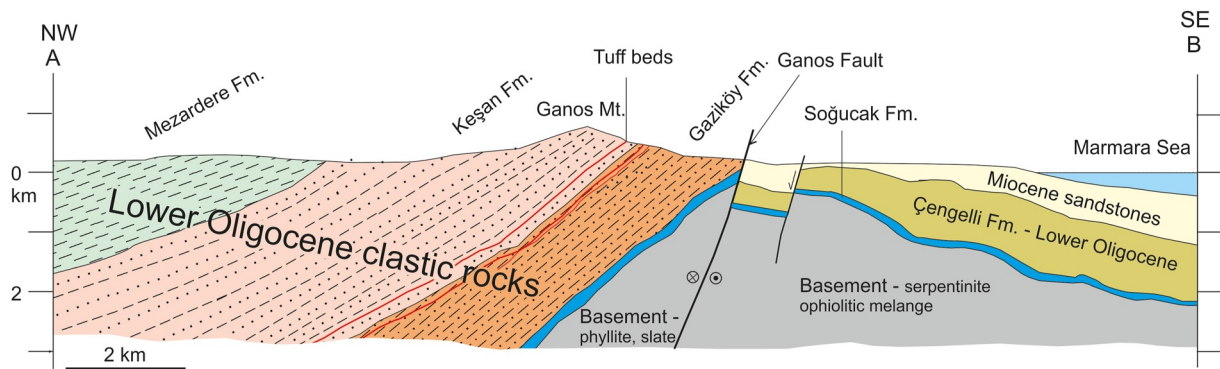
Figure 7. Geological cross-section across the Ganos Mountain, for location of the section see Figure 6.

(Turgut et al., 1991). These show that in the center of the Thrace Basin, the Soğucak Formation is overlain by a thick sequence of sandstone, shale, marl and tuff. This sequence is attributed to the Ceylan Formation and is lithologically similar to the Gaziköy and Keşan formations but also includes marl beds. Bürkan (1992b) has recognized six laterally traceable tuff horizons in the Ceylan Formation, labeled C1 to C6. The tuff horizons can be recognized in sonic logs and can be traced between hydrocarbon wells. We have dated a tuff sample (1926) from the Kumrular-4 oil well in the central Thrace Basin (Figures 2 and 4). The tuff sample comes from a depth of 3,024 m and corresponds to the lowest tuff horizon (C1) of Bürkan (1992b). It occurs a few tens of meters above the limestones of the Soğucak Formation. Seventeen zircon grains yielded an early Oligocene U-Pb age of 31.7 ± 0.2 Ma (Figure 10d, Table S3 in Supporting Information S2). This shows that the Ceylan Formation is the age equivalent of the Gaziköy and Keşan formations (Figure 4) and the late Eocene age assigned to the Ceylan Formation is not correct.

The new zircon ages, supported by limited biostratigraphic data, indicate that the turbidites above the shallow marine limestones of the Soğucak Formation, namely the Gaziköy, Keşan, and Ceylan formations, are of early Oligocene age (34–30 Ma). The period 33–32 Ma was characterized by intensive silicic volcanism in the Rhodope Complex, the largest eruptions originating from the Eastern Rhodope Borovitsa volcano (Figure 1a). The main Borovitsa eruptions occurred at 32.5–32.9 Ma and resulted in ash deposition over a very large area (Marchev et al., 2020), the tuffs close to the contact between the Gaziköy and Keşan formations (32.8 ± 0.3 to 32.2 ± 0.2 Ma, Figure 4) are probably linked to these eruptions. This implies an age of 32.7 ± 0.2 Ma for the contact between the Gaziköy and Keşan formations.

4.4. Lower Oligocene Deltaic Shales—The Mezardere Formation

The turbidites of the Keşan and Ceylan formations pass up into the Mezardere Formation (750 m thick at Ganos Mountain), consisting predominantly of shale with minor sandstone (Figure 8e). A submarine delta front environment is generally accepted for the Mezardere Formation (Gürgey & Batı, 2018; Siyako & Huvaz, 2007; Turgut et al., 1991). East of the town of Keşan, the contact between the Keşan and the overlying Mezardere formations is marked by a prominent tuff layer (Figures 2 and 8d). A sample from this tuff (1992) produced a zircon U-Pb age of 30.1 ± 0.5 (Figure 10a, Table S4 in Supporting Information S1). This tuff layer corresponds to the M1 tuff marking the contact between the Ceylan and overlying Mezardere formations in oil wells and in seismic sections (Bürkan, 1992b). A sandstone sample (1919) from the Mezardere Formation, approximately 70 m above its stratigraphic base, contains two concordant early Oligocene (30.3 ± 0.4 Ma) detrital zircons (Figure 10f, Table S14 in Supporting Information S2), which is compatible with the 30.1 ± 0.5 Ma tuff age from the base of the Mezardere Formation. The Mezardere Formation is also dated as early Oligocene by palynology (Gürgey & Batı, 2018) and shows some microfloral comparison to the Oligocene series on the Black Sea coastal areas (Simmons et al., 2020). Two samples (2064–2065) from the Mezardere Formation in the Ganos section were studied for foraminifera and palynology (Table S1). Sample 2064 contained dinoflagellate cysts (*Glaphyrocysta semitecta*), which indicate an intra early Oligocene age corresponding to zone D14a (33.2–30.2 Ma).

4.5. Oligocene Paralic Sandstones and Mudstones—The Osmancık and Danışmen Formations

The Mezardere Formation passes up into thickly bedded sandstones and mudstones (Figures 4, 6, and 8f), which are attributed to the Osmancık and Danışmen formations (Perinçek et al., 2015; Siyako, 2006a). These formations
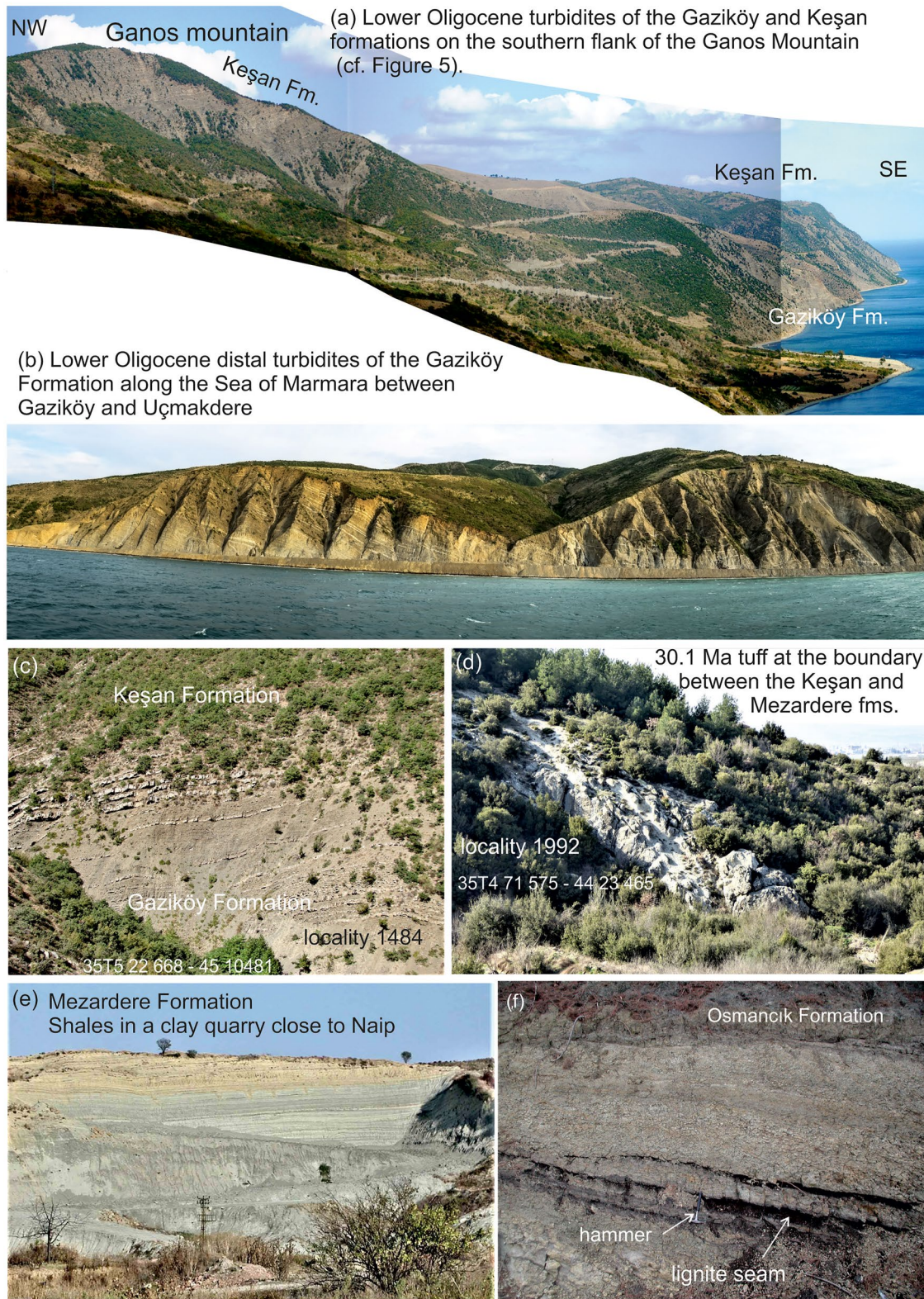
Figure 8. Field photographs from the southern Thrace Basin. (a) Lower Oligocene turbidites of the Gazıköy and Keşan formations on the southeastern flank of the Ganos Mountain (c.f. Figure 6). (b) Distal turbidites of the Gazıköy Formation exposed on the cliffs between Gazıköy and Uçmakdere (c.f. Figure 6). (c) Transition from the distal turbidites of the Gazıköy Formation to the overlying medial turbidites of the Keşan Formation northwest of Güzelköy. (d) The 30.1 Ma tuff layer between the Keşan and Gazıköy formations southeast of Keşan (c.f. Figure 6). (e) Shales of the lower Oligocene Mezardere Formation exposed in a clay quarry close to the village of Naip. (f) Sandstones with lignite seams of the Osmancık Formation close to Barbaros.
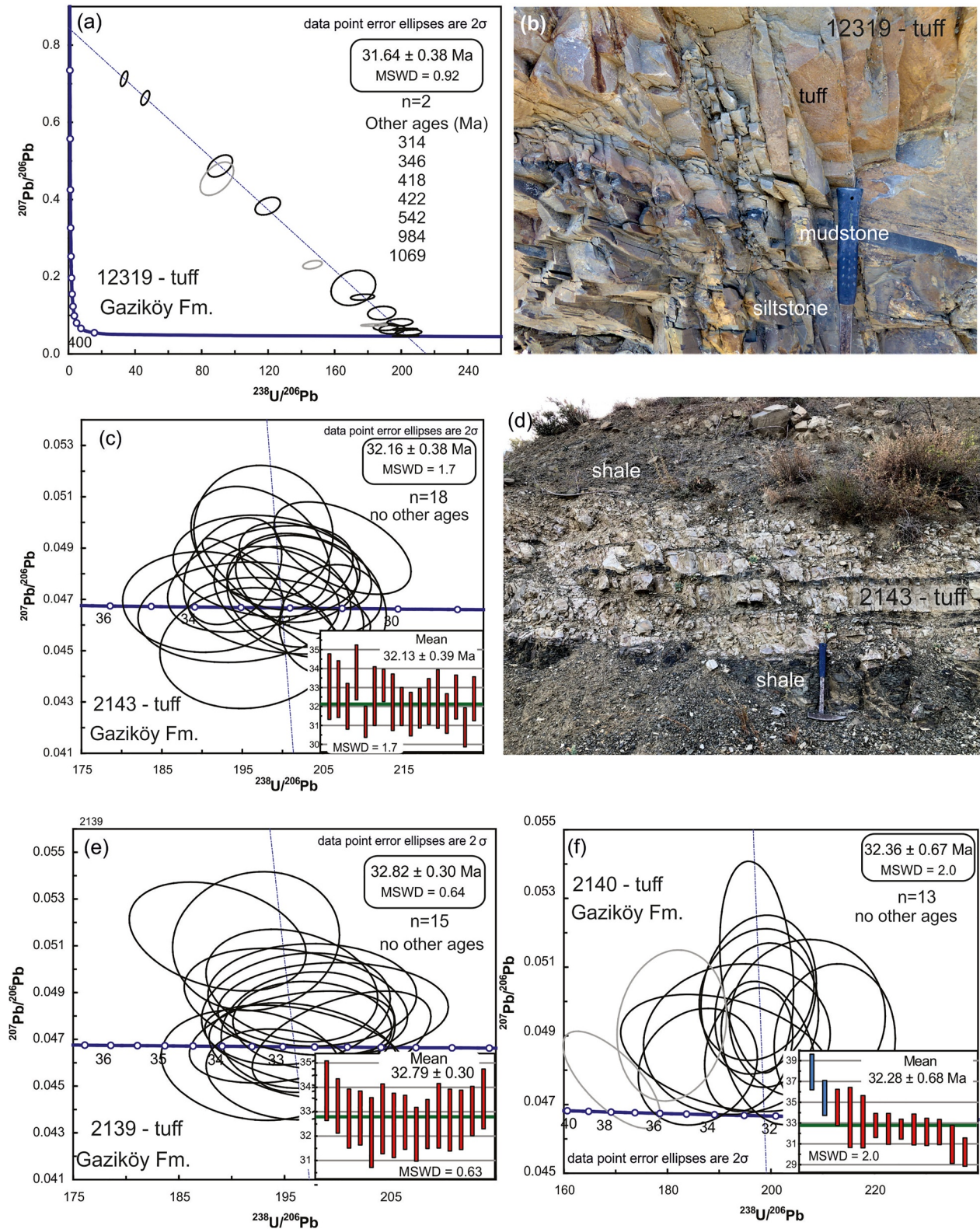
Figure 9. Zircon U-Pb diagrams from the acidic tuffs from the Gaziköy Formation and the photographs of some of the dated tuff layers. For the analytical data see tables in Supporting Information S2 and for the locations of the samples, see Figure 6. The mean ages are at 95% confidence and the box heights are 2σ.
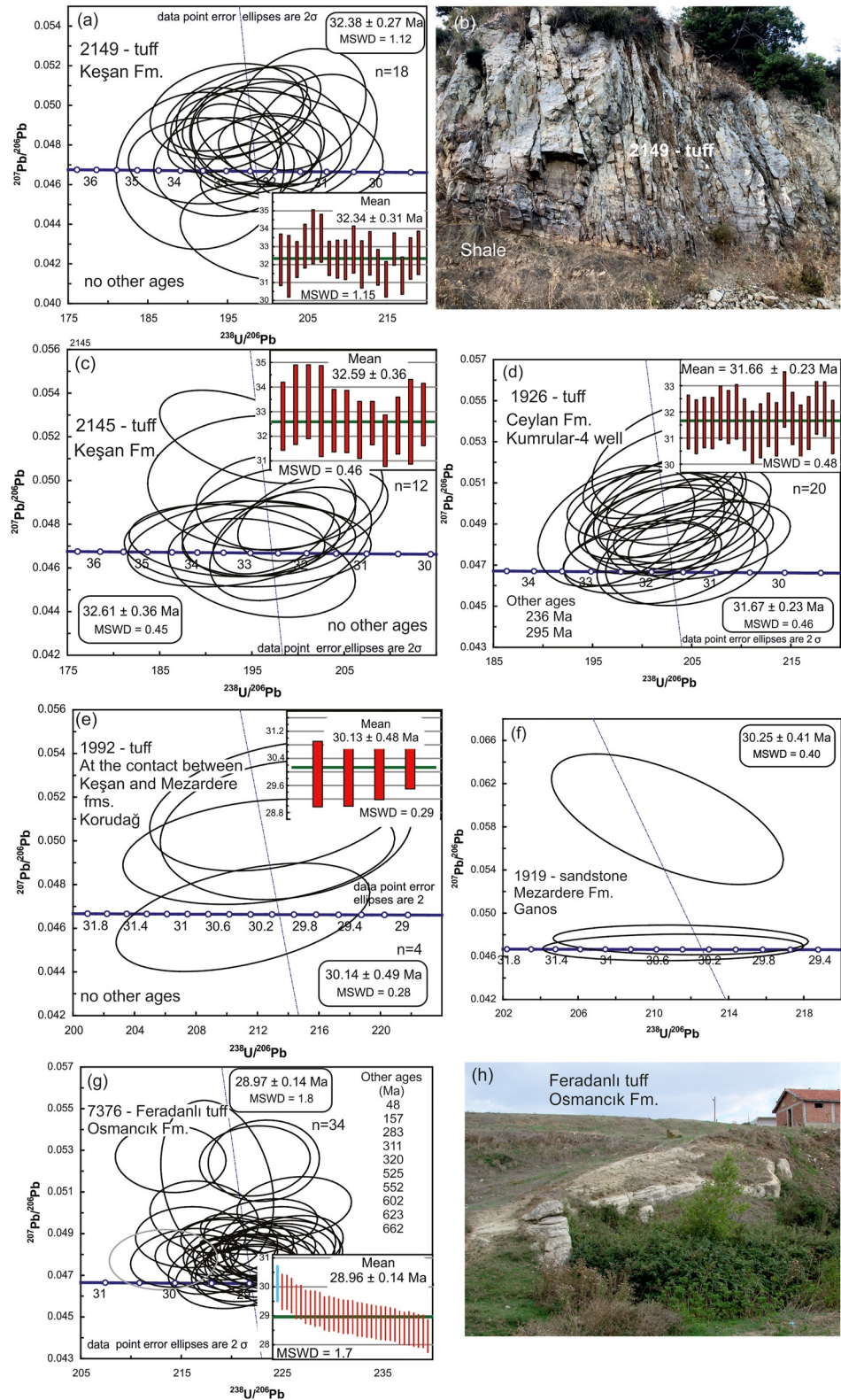
Figure 10. Zircon U-Pb diagrams for the acidic tuffs from the (a, c) Keşan, (d) Ceylan, and (g) Osmancık formations and the photographs of some of the dated tuff layers (b, h). Panel (f) shows the Oligocene ages from the detrital zircons from the Mezardere Formation. For the analytical data see the tables in Supporting Information S2 and for the locations of the samples see Figures 2 and 6. The mean ages are at 95% confidence and the box heights are 2σ.

are lithologically similar and will be described here under the name of Osmancık Formation (min. 500 m thick at Ganos Mountain). The Osmancık Formation was deposited in a deltaic and paralic environment and contains economic lignite deposits (e.g., İslamoğlu et al., 2008; Perinçek et al., 2015). The sandstones of the Osmancık Formation constitute the main gas reservoirs in the Thrace Basin (e.g., Gürgey et al., 2005). The Osmancık Formation represents the terminal depositional stage of the Thrace Basin. It is usually assigned a broad Oligocene age (mostly late Rupelian—early Chattian) based on vertebrate faunas and palynomorphs (Ediger & Alişan, 1989; Lebküchner, 1974; Ozansoy, 1962; Ünay-Bayraktar, 1989), however, many studies also extend its age into the early Miocene (Perinçek et al., 2015; Siyako, 2006a; Turgut & Eseller, 2000; Turgut et al., 1991). We dated zircons from the tuffs from the middle and top parts of the Osmancık Formation. The Feradanlı tuff of Lebküchner (1974) near Tekirdağ, lies stratigraphically about ∼300 m above the shales of the Mezardere Formation (Figures 2 and 6). It is a key horizon, which can be followed for more than 10 km along strike (Figures 6 and 10h, Şentürk et al., 1998). Zircons from a sample (7376) from the Feradanlı tuff yielded a late early Oligocene U-Pb age of 29.0 ± 0.1 Ma (Figure 10g, Table S7 in Supporting Information S2). White porous tuffs, the Çantaköy tuff, constitute the topmost part of the Osmancık Formation southwest of the Çatalca ridge (Figure 2). Zircons from a sample of the Çantaköy tuff gave a latest early Oligocene U-Pb age of 27.9 ± 0.2 Ma (Okay et al., 2019). One sample from the Osmancik Formation (2066), investigated for dinoflagellates yielded the same D14a biozone assemblage as samples from the underlying Mezardere Formation (e.g., sample 2064, Table S1), suggesting reworking of the fauna.

The new zircon ages indicate that the Gaziköy, Keşan, and Mezardere formations are of early Oligocene age (34–29 Ma). Most of the Osmancık Formation is also early Oligocene in age but its age may extend into the early late Oligocene. The initiation of turbidite deposition is constrained to ca. 34 Ma from the upper ages of the Soğucak (38–34 Ma) and Çeltik formations (35–34 Ma), and from the 33–32 Ma tuff ages from the Gaziköy Formation.

The new biostratigraphic data are less precise but mostly do not contradict the early Oligocene ages. Interestingly all the previously published paleontological data (nannoplankton, foraminifera) from the Gaziköy and Keşan formations are Eocene (Aksoy, 1987; Sümengen & Terlemez, 1991; Yıldız et al., 1997) indicating extensive reworking, which is also observed in our samples.

4.6. Eocene—Oligocene Sequence of the Thrace Basin South of the North Anatolian Fault

The Thrace Basin south of the Ganos Fault in the region of Şarköy has a somewhat different stratigraphy than that north of the Fault. South of the Ganos Fault a basement composed of serpentinite, diabase, and Late Cretaceous blueschist crops out along the strands of the North Anatolian fault (Figure 2, Topuz et al., 2008). This basement is unconformably overlain by the late middle to upper Eocene (SBZ18-19) limestones of the Soğucak Formation (E. Özcan et al., 2010). The limestones are in turn overlain by siliciclastic turbidites with calciturbidite beds, debris flow horizons with blocks of serpentinite, gabbro, Eocene limestone, granite in a clastic matrix (Okay et al., 2010). This Çengelli Formation has a minimum thickness of about 600 m and is unconformably overlain by lower-middle Miocene continental sandstones and conglomerates (Figures 6 and 7). Nannoplankton from the Çengelli Formation indicate a general late Priabonian to early Rupelian age range (NP19-22, Okay et al., 2010). During this study we collected four samples from the shales of the Çengelli Formation (samples 2067, 2068, 2074, and 2075) to constrain its age more tightly (Table S1). Foraminifera in sample 2068 indicate an undifferentiated Oligocene age. Samples 2074 and 2075 contain reasonably rich foraminiferal faunas with a ratio of planktonic to benthonic taxa of 60%–70% indicating an upper slope depositional environment. The presence of planktonic foraminifera *Pseudohastigerina naguewichiensis* and probable *Turborotalia increbescens* (supported by the presence of *Chiloguembelina cubensis*) indicate biozone O1 (sensu Wade et al., 2011) corresponding to the lower part of the early Oligocene (approximately 33.9–32.1 Ma according to Speijer et al. (2020)). Sample 2075 gave a generalized early Oligocene age based on palynology (*Glaphyrocysta semitecta*, *Hemiplacophora semilunifera*, *Lentinia serra*, and *Achomosphaera alcicornu*). Paleontological data therefore indicate an early Oligocene age for the turbidites south of the Ganos Fault.

5. Sedimentation Rates in the Thrace Basin

The new ages from the tuffs allow a precise estimation of the clastic sedimentation rates in the Ganos region of the Thrace Basin. The thickness of the limestones at the base of the Thrace Basin *s.s.* (the Soğucak Formation) ranges

from 15 to 40 m (E. Özcan et al., 2010) and its age ranges from 38 to 34 Ma (late Bartonian—Priabonian). The sudden subsidence above these limestones is best observed north of the Saros Bay, where a 30-m-thick sequence of latest Eocene (35–34 Ma) pelagic limestones (Çeltik Formation) lie over the shallow marine limestones of the Soğucak Formation (Erbil et al., 2021). Thus, the subsidence in the Thrace Basin started at ca. 34 Ma close to the Eocene-Oligocene boundary (Figure 11a). In the Ganos region the uppermost Eocene limestones must have been overlain by the distal turbidites of the Gaziköy Formation, however, the contact is not exposed (Figure 5). The Gaziköy Formation has a minimum thickness of 855 m (Okay et al., 2004). There are several tuff layers close to the contact between the Gaziköy and the overlying Keşan formations, which have ages between 32.2 ± 0.6 and 32.8 ± 0.3 Ma (Table 1). These ages correspond to the large Borivitsa eruptions in the eastern Rhodopes dated to 32.5–32.9 Ma (Marchev et al., 2020). Thus an age of 32.7 ± 0.2 Ma is taken for the transitional boundary between the Gaziköy and Keşan formations (Figure 8c). The turbidites of the Keşan Formation have a thickness of about 3.2 km (Okay et al., 2004). The contact between the Keşan Formation the overlying shales and minor sandstones of the Mezardere Formation is marked by a prominent tuff layer (Figure 2), which is dated in this study to 30.1 ± 0.5 Ma (Figure 10e). The Lower Oligocene Mezardere Formation is 750 m thick in the Ganos region (Okay et al., 2004); similar or greater thickness for the Mezardere Formation are reported from the other parts of the Thrace Basin (e.g., Gürgey & Batı, 2018; Siyako, 2006b; Siyako & Huvaz, 2007). The Mezardere Formation is overlain by the paralic sandstones and shales of the Osmancık Formation. In the Ganos region the Osmancık Formation is eroded on top and is about 500 m thick; in the central parts of the Thrace region, its thickness reaches 1.5 km (Perinçek et al., 2015; Siyako, 2006b). In the Ganos region, the Feradanlı tuff, which lies 300 m above the Mezardere-Osmancık contact, is dated to 29.0 ± 0.1 Ma (Figure 10g), and provides another time marker for the subsidence curve (Figure 11a). The top age of the Osmancık Formation is poorly defined in the Ganos region. In the eastern part of the Thrace Basin in the Çatalca region, a tuff layer close to the top of the Osmancık Formation yielded a U-Pb zircon age of 27.9 ± 0.2 Ma (Okay et al., 2019). A similar age is assumed for the upper part of the Osmancık Formation (Figure 11a).

The thickness and age constraints indicate fast sediment accumulation rates of 1.0 km/my (1.0 mm/yr) between 34 and 28 Ma. The accumulation rates are on the high end of the spectra (e.g., Allen & Allen, 2013) and imply fast creation of accommodation space between 34 and 28 Ma. The calculations are based on present sedimentary thickness; a subsidence analysis will also involve sediment compaction, paleobathymetry and sea level changes (e.g., Allen & Allen, 2013; Xie & Heller, 2009). Among these factors, reduction of porosity with burial depth has the largest effect, therefore, the sediment accumulation curve in Figure 11 represents a minimum subsidence curve.

Previous estimates on the burial history of the Thrace Basin (e.g., Huvaz et al., 2005, 2007) used similar thicknesses but assumed much longer burial times (30 Myr) compared to the present study (6 Myr).

6. Provenance of the Thrace Basin—Detrital Zircons

Paleocurrent data from the Thrace Basin indicate eastward flow in the western and central parts and northward flow in the south (Figure 2, Caracciolo et al., 2015; Cavazza et al., 2013; d'Atri et al., 2012; Maravelis et al., 2016; Şenol, 1980). Sandstones from the western and central parts of the Thrace Basin are characterized by plutonic-metamorphic detritus with a likely source in the Rhodope Complex, whereas those from the southern part have an additional ophiolite and penecontemporaneous volcanic detrital component and indicate a source in the south (Caracciolo et al., 2015; Cavazza et al., 2013; d'Atri et al., 2012; Maravelis et al., 2016; Okay et al., 2010). To further constrain the provenance of the sediments of the Thrace Basin, we analyzed detrital zircons from three sandstone samples from the Ganos Mountain, one each from the Gaziköy, Keşan, and Mezardere formations (Figures 4 and 6). The petrography and heavy mineral composition of sandstones from these formations are described in detail by d'Atri et al. (2012), who differentiate two petrofacies regions: the northern and southern petrofacies separated by the North Anatolian Fault. Our samples come from the northern petrofacies, where sandstones are characterized by an absence of carbonate and volcanic grains, and east-directed paleocurrents, whereas carbonate and volcanic grains are common in the sandstones of the southern petrofacies, which show north-directed paleocurrents.

Detrital zircons from all three samples show a similar age pattern characterized by the dominance of Late Carboniferous, late Neoproterozoic—early Paleozoic, Late Ordovician, and Late Jurassic zircons (Figure 12). Abbo et al. (2020) provide detrital zircon ages from modern beach sands at the ends of three Rhodopian rivers
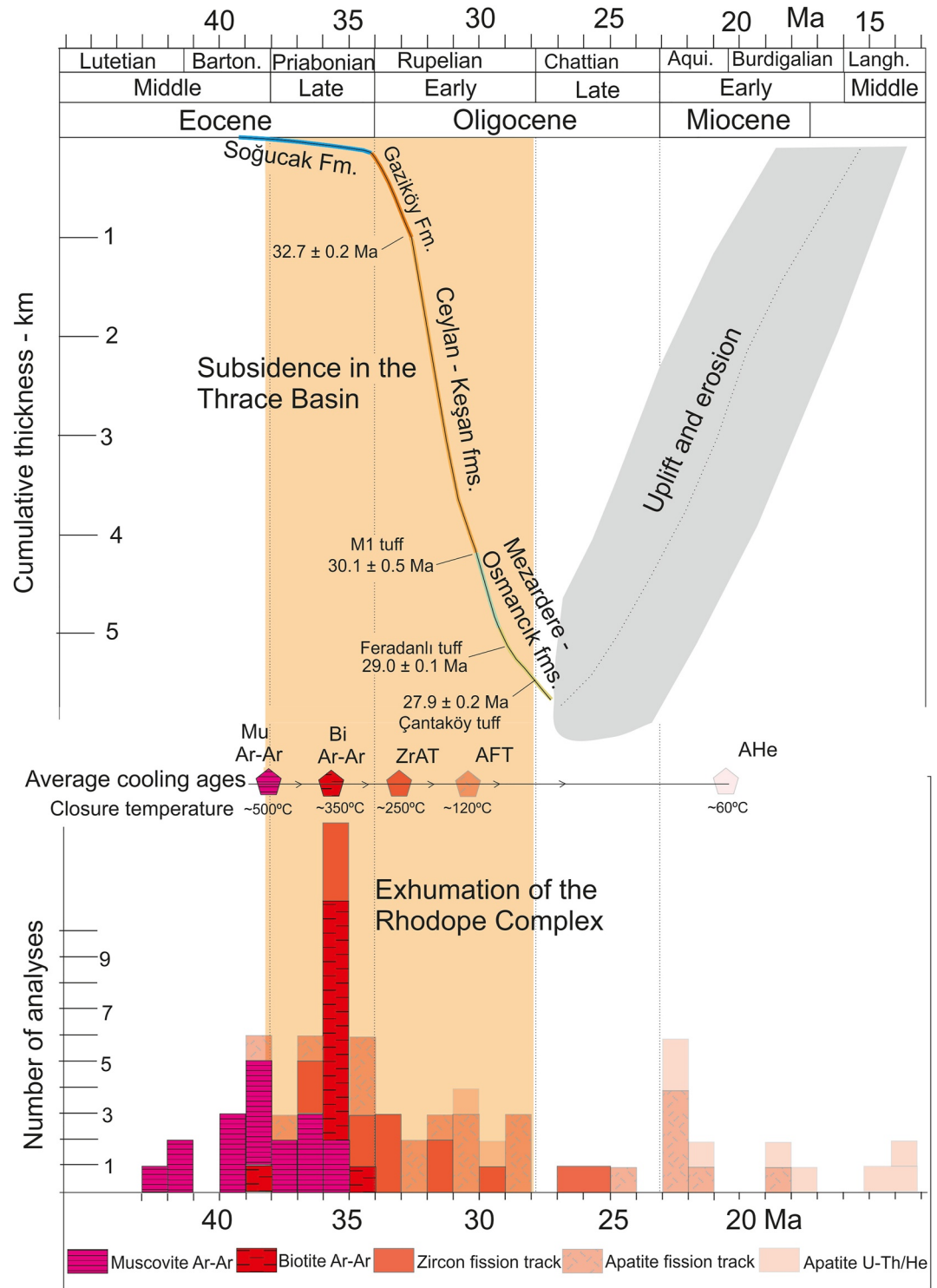
Figure 11. (a) Sediment accumulation in the Thrace Basin based on uncompacted sediment thickness in Ganos Mountain. (b) Thermochronological data from the northern Rhodope Complex compiled from Bonev et al. (2006, 2013), Lips et al. (2000), Márton et al. (2010), Kaiser-Rohrmeier et al. (2013), and Kounov et al. (2015, 2020). See Table S15 for the summary of the thermochrological data.
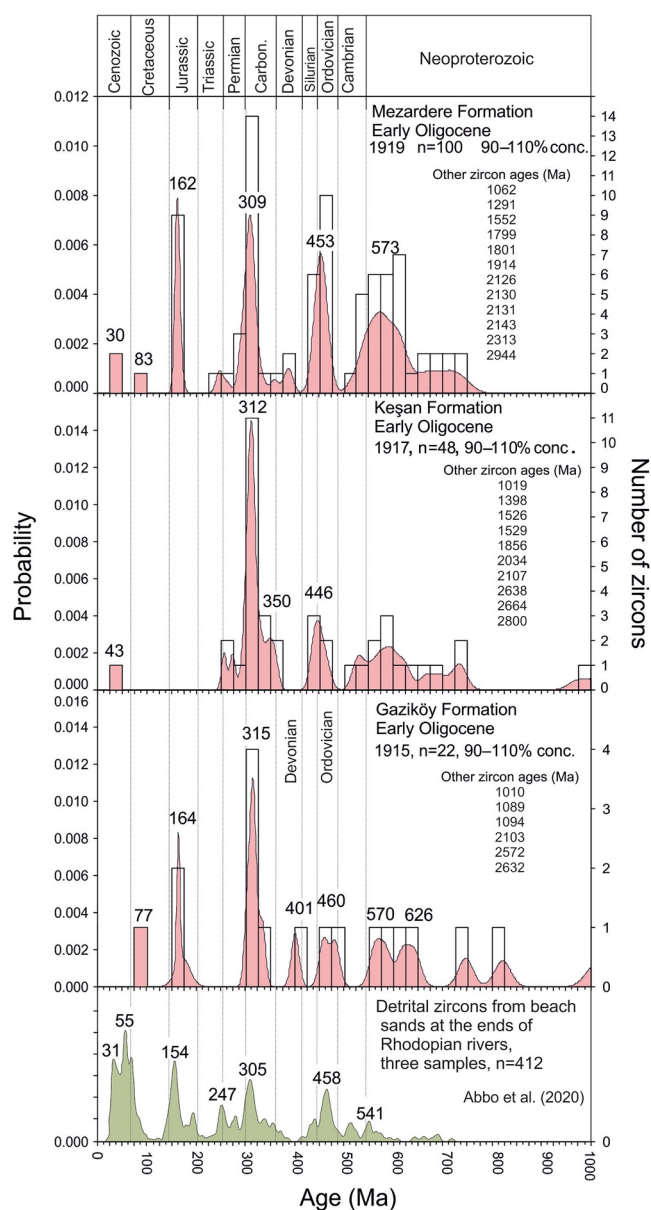
Figure 12. Detrital U-Pb zircon ages from three lower Oligocene sandstones from the Thrace Basin shown in relative probability plot histograms. For the analytical data see the Tables S12–S14 in Supporting Information S2. The bottom panel shows the detrital zircons ages from the mouths of the Rhodopian rivers after Abbo et al. (2020).

(Figure 12). Their age spectra are comparable to those from the Thrace Basin with similar Late Jurassic, Late Carboniferous, and Devonian age peaks. Carboniferous and late Neoproterozoic—early Paleozoic granites are common in the Pontides, and are also present in the Rhodope Complex and in the Anatolide-Tauride Block, thus they are not diagnostic (e.g., Burg, 2012; Okay & Kylander-Clark, 2023). On the other hand, Late Ordovician (460–446 Ma) metagranites are widely reported from the Rhodope Complex (c.f. Bonev et al., 2019) but are rare in the Pontides (c.f. Akdoğan et al., 2021). The Jurassic zircons are especially diagnostic since Jurassic granites are unknown from the Strandja Massif and from the Balkans but are reported from the Rhodope Complex (Georgiev et al., 2016; Turpaud & Reischmann, 2010). Burg (2012) even suggests the presence of a Late Jurassic magmatic arc in the Rhodopes. The absence of early Eocene zircon ages in the Thrace Basin, in contrast to their prominence in the modern river sediments indicates that the Eocene granites of the Rhodope Complex and those south of the Marmara Sea were not exposed by the early Oligocene. Thus, detrital zircon populations of the sandstones from the Gaziköy, Keşan, and Mezardere formations are compatible with a source in the Rhodope Complex. It is interesting that only three out of 170 detrital zircon ages from three lower Oligocene sandstone samples are Cenozoic (Figure 12). This implies that the Oligocene volcanic centers in the northern Rhodopes did not provide any detritus to the Ganos region, and the tuffs within the Ganos sequence represent airfall volcanic ash. However, with increase in the number of sandstone samples and number of zircons dated, Cenozoic zircons could be shown to be more common, especially in the southern lithofacies belt of d'Atri et al. (2012).

7. The Rhodope Complex and the Thrace Basin

The Rhodope Complex is a large area of high-grade metamorphic rocks and Cenozoic granites in northeastern Greece and Bulgaria (Figure 1). It has an unusually long thermal history involving several stages of metamorphism. High-grade metamorphism, including high- to ultra-high pressure metamorphism, probably took place in the Middle to Late Jurassic (170–140 Ma) followed by amphibolite-facies metamorphism, which lasted until the early Eocene (Bonev et al., 2010; Burg, 2012; Wawrzenitz et al., 2015). The metamorphic rocks are intruded by a series of Cenozoic granites (Figure 1). Thermochronological data from the northern Rhodope Complex, the region northeast of the Nestos thrust, are compiled in Table S15 and are shown in Figure 11b (Bonev et al., 2006, 2013; Kaiser-Rohrmeier et al., 2013; Kounov et al., 2015, 2020; Lips et al., 2000; Márton et al., 2010). Average muscovite Ar-Ar, biotite Ar-Ar, zircon fission track and AFT ages from the northern Rhodope Complex are 38, 36, 33, and 30 Ma respectively and indicate late Eocene to early Oligocene exhumation (Figure 11b, Table S14 in Supporting Information S2). These data show that the exhumation of the northern Rhodope Complex was coeval with subsidence (34–28 Ma) in the Thrace

Basin (Figure 11). Furthermore, the regional NE-SW extension direction during the exhumation of the Rhodope Complex, as indicated by the mineral stretching lineations, is perpendicular to the axis of the maximum sedimentary thickness in the Thrace Basin (Figure 1). These temporal and spatial relationships, as well as the Rhodope Complex as a major source for the Thrace Basin, indicate a genetic connection between the exhumation of the Rhodope Complex and formation of the Thrace Basin.

Although several extensional shear zones have been described from within the northern Rhodope Complex, there are no major thermal breaks across these shear zones; the major jump in cooling ages occurs between the Rhodope Complex and the tectonically overlying Circum-Rhodope Complex (Figure 1). The latter consist of low-grade metamorphic rocks with Jurassic and early Cretaceous depositional ages (e.g., Bonev & Stampfli, 2003, 2011;

Meinhold & Kostopoulos, 2013). The regional metamorphism in the Circum-Rhodope Complex is probably Cretaceous in age and the metamorphic rocks are unconformably overlain by upper Eocene conglomerates and limestones of the Thrace Basin (e.g., Chatalov et al., 2015; Kopp, 1965; Okay et al., 2010). The exhumation of the northern Rhodope Complex was principally related to the Circum-Rhodope extensional shear zone between the Rhodope and Circum-Rhodope complexes (Figures 5d and 5e).

8. Rotational Mode of Opening of the Thrace Basin

Based on the paleomagnetically determined Cenozoic clockwise rotations in the northern Aegean (e.g., Dimitriadis et al., 1998), Brun and Sokoutis (2007) suggested a rotational exhumation of the Rhodope Complex. We suggest that this clockwise rotation also led to the opening of the Thrace Basin during the latest Eocene—Oligocene. The evidence for the rotational opening of the Thrace Basin includes: (a) The axis of major subsidence in the Thrace Basin trends NW-SE perpendicular to the Cenozoic paleomagnetic rotations (Figure 1a). (b) The triangular shape of the Thrace Basin tapering toward northwest (Figure 1). (c) The NE-SW trending arcuate stretching lineations in the Rhodope. A rotation of 12°, estimated by Dimitriadis et al. (1998), would produce an 80 km extension in the outer rim of an arc with a radius of 350 km in the southern Balkans (Figure 5d). The western margin of the Strandja Massif would form the eastern end of the area undergoing extension, and the outer rim of the arc would correspond to the southern margin of the Thrace Basin.

The Oligocene extension does not extend south of the Marmara Sea, where with the exception of the northern margin of the Biga Peninsula, the late Eocene and Oligocene time was a period of non-deposition (Figure 1, Okay et al., 2020). Oligocene uplift and erosion in this region are also indicated by AFT and apatite (U-Th)/He ages (Figure 2, Zattin et al., 2010). The termination of extension south of the Marmara Sea requires kinematically the presence of a sinistral strike-slip fault zone (Figure 5d). The North Anatolian Fault, a late Miocene dextral strike-slip fault, largely follows the position of this hypothetical fault. Zattin et al. (2005, 2010) has provided thermochronological evidence for the Oligocene activity along the North Anatolian Fault in southern Thrace. The Cenozoic ductile shear zones described in the Eocene granites from the Marmara Island from the northern margin of the Kapıdağ peninsula (Figure 2) could represent segments of this sinistral fault (Figure 2). Both of these granites have middle Eocene (48–47 Ma) crystallization (Okay et al., 2022) and Oligocene (33 and 27 Ma) AFT ages (Zattin et al., 2010). The shear zone on the northern margin of the Kapıdağ peninsula is described either as sinistral (Aksoy, 1998) or dextral (Türkoğlu et al., 2016).

9. Origin of the Thrace Basin

The Thrace Basin has been regarded variously as an intramontane (Doust & Arıkan, 1974; Perinçek, 1991), a forearc (Görür & Okay, 1996; Maravelis et al., 2016; Saner, 1980), orogenic collapse (Cavazza et al., 2013) or supradetachment basin (e.g., Kilias et al., 2013). The triangular shape of the basin and the presence of thick marine sequences are unlike those of intramontane basins. Although the Thrace Basin lies stratigraphically on an accretionary complex in the south (e.g., Okay et al., 2010), there is no evidence for ongoing subduction during the late Eocene and later under of the Thrace Basin, as pointed out by Cavazza et al. (2013). Fore-arc basins are dominated by contemporaneous volcanic detritus derived from the magmatic arc, as for example, the Great Valley basin in California (e.g., DeGraaff-Surpless et al., 2002) or the Late Cretaceous forearc basins in the Pontides (Okay & Kylander-Clark, 2023). In contrast, volcanic detritus is limited in the sandstones of the Thrace Basin, especially in the region north of the Ganos Fault, and there are hardly any Tertiary detrital zircons in the studied sandstone samples. An orogenic collapse basin would require a thick crust prior to extension. However, the presence of lower Eocene sequences in the center of the Thrace Basin is not compatible for a thick crust during the Eocene. Small sub-basins within and adjacent to the Rhodope Complex might have formed above detachment faults (Burchfiel et al., 2003; Márton et al., 2010), however, several features of the Thrace Basin are unlike those seen in the supra-detachment basins (e.g., Friedmann & Burbank, 1995) including (a) its size of 200 km by 200 km, (b) general absence of syn-sedimentary faulting as revealed in seismic sections, and (c) absence of extensional shear zones below the basinal sediments; wherever observed, the basal beds of the Thrace Basin lie unconformably over the basement. We suggest that the Thrace Basin was formed by clockwise crustal rotation as explained in the previous section. Large normal faults between the metamorphic rocks of the Strandja Massif and Oligocene sediments of the Thrace Basin, imaged in the seismic sections (Okay et al., 2019; Turgut

& Eseller, 2000; Turgut et al., 1991), formed the northeastern margin of the rotating block (Figure 5d). The Circum-Rhodope shear zone formed its western margin.

The exhumation of the northern Rhodope Complex was coeval with the main subsidence in the Thrace Basin. Furthermore, although more than 10 km of crustal section is removed from the top of the Rhodope Complex, its present crustal thickness (50 km) is considerably more than that underneath the Thrace Basin (28–30 km), which suggests crustal flow from the base of the Thrace Basin to the Rhodope Complex during the early Oligocene (Figure 5e). A similar opening mechanism involving crustal flow is suggested for the super-deep South China basins (e.g., Clift, 2015; Dong et al., 2020). Thermal subsidence following the cessation of the fault activity led to the sedimentation over a wider area in the Thrace region and concealed most of the syn-exhumation structures.

10. Conclusions

New biostratigraphic, geochronological and geological data and critical appraisal of literature lead to a number of conclusions with regard to the origin and development of the Thrace Basin.

1. The Thrace region comprises three sedimentary sequences separated by major unconformities; these are (a) Lower-middle Eocene, (b) Middle/upper Eocene—Oligocene, and (c) Miocene-Pliocene (Figure 3). Lower-middle Eocene and Miocene-Pliocene sequences are also widespread in the rest of northwest Anatolia, and only the middle/upper Eocene—Oligocene sequence is specific to the Thrace Basin (Figure 1). As an individual depocenter the Thrace Basin is mainly of late Eocene-Oligocene age.
2. Over 95% of the upper Eocene—Oligocene sequence of the Thrace Basin consists of siliciclastic rocks; in previous studies this sequence was assigned an early Eocene to late Oligocene age. New zircon U-Pb ages from the tuffs (Figures 7 and 8) and new biostratigraphic data show that the bulk of the clastic sequence (>90%) is of early Oligocene age (34–28 Ma).
3. Early Oligocene in the Thrace Basin is characterized by high turbidite depositional rates of 1.0 km/my (Figure 11a).
4. New detrital zircon ages (Figure 12) and published paleocurrent and petrographic data indicate that the sediment to the Thrace Basin was derived from the west from the Rhodope Complex and from the south.
5. Crustal extension and rapid subsidence in the Thrace Basin (34–28 Ma) occurred at the same time as the exhumation of the northern Rhodope Complex (36–28 Ma) suggesting a genetic link between these two events (Figure 11).
6. Paleomagnetic evidence for the Oligocene clockwise rotation of the southern Balkans, arcuate stretching lineations in the Rhodope Complex and the triangular shape of the Thrace Basin (Figure 1) indicate that the opening of the Thrace Basin was linked to clockwise rotation in the northern Aegean (Figure 5d), possibly associated with lower crustal flow from the base of the Thrace Basin to the Rhodope Complex (Figure 5e).
7. Thermal models of the Thrace Basin assume deposition from early Eocene until early middle Miocene (from 53 to 15 Ma, Hoşgörmez & Yalçın, 2005; Huvaz et al., 2005, 2007), whereas the sedimentation was restricted to a much narrower interval (34–28 Ma). The very fast burial history requires modification in the parameters for oil and gas generation in the Thrace Basin.

Data Availability Statement

Original data generated from this study are openly available in Okay (2023) on the Mendeley database (https://data.mendeley.com/datasets/hy3s7bm97k/1).

References

Abbo, A., Avigad, D., & Gerdes, A. (2020). Crustal evolution of peri-Gondwana crust into present day Europe: The Serbo-Macedonian and Rhodope massifs as a case study. *Lithos*, *356*, 105295. https://doi.org/10.1016/j.lithos.2019.105295

Akbayram, K., Okay, A. I., & Satır, M. (2013). Early Cretaceous closure of the Intra-Pontide Ocean in western Pontides (northwestern Turkey). *Journal of Geodynamics*, *65*, 38–55. https://doi.org/10.1016/j.jog.2012.05.003

Akbayram, K., Sorlien, C., & Okay, A. I. (2016). Evidence for a minimum 52±1 km of total offset along the northern branch of the North Anatolian Fault in northwest Turkey. *Tectonophysics*, *668–669*, 35–41. https://doi.org/10.1016/j.tecto.2015.11.026

Akdoğan, R., Hu, X., Okay, A. I., Topuz, G., & Xue, W. (2021). Provenance of the Paleozoic to Mesozoic siliciclastic rocks of the Istanbul zone constrains the timing of the Rheic Ocean closure in the eastern Mediterranean region. *Tectonics*, *40*(12), e2021TC006824. https://doi.org/10.1029/2021tc006824

Aksoy, R. (1998). Strain analysis of the Kapıdağı Peninsula shear zone in the Ocaklar granitoid, NW Turkey. *Turkish Journal of Earth Sciences*, *7*, 79–85.

Aksoy, Z. (1987). Depositional environment of the units in the Barbaros-Keşan-Kadıköy-Gaziköy area (southern Thrace) (in Turkish). In *Proceedings of the 7th Petroleum Congress of Turkey* (pp. 292–311).

Allen, P. A., & Allen, J. R. (2013). *Basin analysis: Principles and application to petroleum play assessment* (3rd ed.). Wiley.

Altunkaynak, Ş., Sunal, G., Aldanmaz, E., Genç, C. Ş., Dilek, Y., Furnes, H., et al. (2012). Eocene Granitic Magmatism in NW Anatolia (Turkey) revisited: New implications from comparative zircon SHRIMP U–Pb and ^{40}Ar–^{39}Ar geochronology and isotope geochemistry on magma genesis and emplacement. *Lithos*, *155*, 289–309. https://doi.org/10.1016/j.lithos.2012.09.008

Armijo, R., Meyer, B., Hubert, A., & Barka, A. (1999). Westward propagation of the North Anatolian fault into the northern Aegean: Timing and kinematics. *Geology*, *27*(3), 267–270. https://doi.org/10.1130/0091-7613(1999)027<0267:wpotna>2.3.co;2

Armstrong, H. A., & Brasier, M. D. (2005). *Microfossils*. Blackwell Publishing Ltd (Wiley-Blackwell). https://doi.org/10.1002/9781118685440

Baykal, A. F. (1943). La géologie de la région de Şile (Bithynie-Anatolie). *Istanbul Üniversitesi Fen Fakültesi Monografileri*, *3*, 233.

Baykal, A. F., & Önalan, M. (1980). Şile sedimentary melange (Şile Olistostrome) (in Turkish). In *Proceedings of the Altınlı Symposium* (pp. 15–25). Türkiye Jeoloji Kurumu.

Bayrak, M., Gürer, A., & Gürer, Ö. F. (2004). Electromagnetic imaging of the Thrace Basin and intra-Pontide subduction zone, northwestern Turkey. *International Geology Review*, *46*(1), 64–74. https://doi.org/10.2747/0020-6814.46.1.64

Black, L., Kamo, S., Allen, C., Davis, D., Aleinikoff, J., Valley, J., et al. (2004). Improved ^{206}Pb/^{238}U microprobe geochronology by the monitoring of a trace-element-related matrix effect; SHRIMP, ID–TIMS, ELA–ICP–MS and oxygen isotope documentation for a series of zircon standards. *Chemical Geology*, *205*(1–2), 115–140. https://doi.org/10.1016/j.chemgeo.2004.01.003

Bonev, N., Filipov, P., Raicheva, R., Chiaradia, M., & Moritz, R. (2019). Detrital zircon age and Sr isotopic constraints for a Late Palaeozoic carbonate platform in the lower Rhodope thrust system, Pirin, SW Bulgaria. *Geological Magazine*, *156*(12), 2117–2124. https://doi.org/10.1017/s0016756819001183

Bonev, N., Marchev, P., & Singer, B. (2006). 40Ar/39Ar geochronology constraints on the Middle Tertiary basement extensional exhumation, and its relation to ore-forming and magmatic processes in the Eastern Rhodope (Bulgaria). *Geodinamica Acta*, *19*(5), 267–282. https://doi.org/10.3166/ga.19.267-282

Bonev, N., Moritz, R., Márton, I., Chiaradia, M., & Marchev, P. (2010). Geochemistry, tectonics, and crustal evolution of basement rocks in the Eastern Rhodope Massif, Bulgaria. *International Geology Review*, *52*(2–3), 269–297. https://doi.org/10.1080/00206810802674493

Bonev, N., Spikings, R., Moritz, R., Marchev, P., & Collings, D. (2013). ^{40}Ar/^{39}Ar age constraints on the timing of Tertiary crustal extension and its temporal relation to ore-forming and magmatic processes in the Eastern Rhodope Massif, Bulgaria. *Lithos*, *180–181*, 264–278. https://doi.org/10.1016/j.lithos.2013.05.014

Bonev, N., & Stampfli, G. (2011). Alpine tectonic evolution of a Jurassic subduction accretionary complex: Deformation, kinematics and ^{40}Ar/^{39}Ar age constraints on the Mesozoic low-grade schists of the circum-Rhodope belt in the eastern Rhodope-Thrace region, Bulgaria-Greece. *Journal of Geodynamics*, *52*(2), 143–167. https://doi.org/10.1016/j.jog.2010.12.006

Bonev, N. G., & Stampfli, G. M. (2003). New structural and petrologic data on Mesozoic schists in the Rhodope (Bulgaria): Geodynamic implications. *Comptes Rendus Geoscience*, *335*(8), 691–699. https://doi.org/10.1016/s1631-0713(03)00122-6

Boyanov, I., & Goranov, A. (2001). Late Alpine (Palaeogene) superimposed depressions in parts of southeast Bulgaria. *Geologica Balcanica*, *31*(3–4), 3–36. https://doi.org/10.52321/geolbalc.31.3-4.3

Brun, J.-P., & Sokoutis, D. (2007). Kinematics of the southern Rhodope core complex (north Greece). *International Journal of Earth Sciences*, *96*(6), 1079–1099. https://doi.org/10.1007/s00531-007-0174-2

Burchfiel, B. C., Nakov, R., Dumurdzanov, N., Papanikolaou, D., Tzankov, T., Serafimovski, T., et al. (2008). Evolution and dynamics of the Cenozoic tectonics of the South Balkan extensional system. *Geosphere*, *4*(6), 919–938. https://doi.org/10.1130/ges00169.1

Burchfiel, B. C., Nakov, R., & Tzankov, T. (2003). Evidence from the Mesta half-graben, SW Bulgaria, for the late Eocene beginning of Aegean extension in the central Balkan Peninsula. *Tectonophysics*, *375*(1–4), 61–76. https://doi.org/10.1016/j.tecto.2003.09.001

Burg, J.-P. (2012). Rhodope: From Mesozoic convergence to Cenozoic extension. Review of petro-structural data in the geochronological frame. *Journal of the Virtual Explorer*, *42*, 1–44. https://doi.org/10.3809/jvirtex.2011.00270

Bürkan, K. (1992a). Geochemical evaluation of the Thrace Basin (in Turkish). In *Proceedings of the 9th Petroleum Congress of Turkey* (pp. 34–48).

Bürkan, K. (1992b). *The stratigraphic position, distribution and hydrocarbon potential of the tuffs in the Thrace Basin (in Turkish)* (p. 43). Turkish Petroleum Corporation (TPAO) Exploration Division.

Caracciolo, L., Critelli, S., Cavazza, W., Meinhold, G., von Eynatten, H., & Manetti, P. (2015). The Rhodope zone as a primary sediment source of the southern Thrace basin (NE Greece and NW Turkey): Evidence from detrital heavy minerals and implications for central-eastern Mediterranean palaeogeography. *International Journal of Earth Sciences*, *104*(3), 815–832. https://doi.org/10.1007/s00531-014-1111-9

Cattò, S., Cavazza, W., Zattin, M., & Okay, A. I. (2018). No significant Alpine-age tectonic overprint of the Cimmerian Strandja Massif (SE Bulgaria and NW Turkey). *International Geology Review*, *60*(4), 513–529. https://doi.org/10.1080/00206814.2017.1350604

Cavazza, W., Caracciolo, L., Critelli, S., d'Atri, A., & Zuffaa, G. G. (2013). Petrostratigraphic evolution of the Thrace Basin (Bulgaria, Greece, Turkey) within the context of Eocene-Oligocene post-collisional evolution of the Vardar-İzmir-Ankara suture zone. *Geodinamica Acta*, *26*(1–2), 27–55. https://doi.org/10.1080/09853111.2013.858943

Chatalov, A., Ivanova, D., & Bonev, N. (2015). Transgressive Eocene clastic-carbonate sediments from the circum-Rhodope belt, northeastern Greece: Implications for a rocky shore palaeoenvironment. *Geological Journal*, *50*(6), 799–810. https://doi.org/10.1002/gj.2598

Clift, P. D. (2015). Coupled onshore erosion and offshore sediment loading as causes of lower crust flow on the margins of South China Sea. *Geoscience Letters*, *2*, 1–13. https://doi.org/10.1186/s40562-015-0029-9

Costa, L. I., & Manum, S. B. (1988). The description of the interregional zonation of the Paleogene. In R. Vinken (Ed.), *The Northwest European tertiary basin* (pp. 321–330). Geologisches Jahrbuch A, no. 100.

d'Atri, A., Zuffa, G. G., Cavazza, W., Okay, A. I., & Di Vincenzo, G. (2012). Detrital supply from subduction/accretion complexes to the Eocene–Oligocene post-collisional southern Thrace Basin (NW Turkey and NE Greece). *Sedimentary Geology*, *243–244*, 117–129. https://doi.org/10.1016/j.sedgeo.2011.10.008

DeGraaff-Surpless, K., Graham, S. A., Wooden, J. L., & McWilliams, M. O. (2002). Detrital zircon provenance analysis of the Great Valley Group, California: Evolution of an arc-forearc system. *Geological Society of America Bulletin*, *114*(12), 1564–1580. https://doi.org/10.1130/0016-7606(2002)114<1564:dzpaot>2.0.co;2

Dimitriadis, S., Kondopoulou, D., & Atzemoglou, A. (1998). Dextral rotations and tectonomagmatic evolution of the southern Rhodope and adjacent regions (Greece). *Tectonophysics*, *299*(1–3), 159–173. https://doi.org/10.1016/s0040-1951(98)00203-0

Dong, M., Zhang, J., Brune, S., Wu, S., Fang, G., & Yu, L. (2020). Quantifying postrift lower crustal flow in the northern margin of the South China Sea. *Journal of Geophysical Research: Solid Earth*, *125*(2), e2019JB018910. https://doi.org/10.1029/2019jb018910

Doust, H., & Arıkan, Y. (1974). The geology of the Thrace Basin. In *Proceedings of the 2nd Petroleum Congress of Turkey* (pp. 119–136).

Ediger, V., & Alişan, C. (1989). Tertiary fungal and algal palynomorph biostratigraphy of the northern Thrace Basin, Turkey. *Review of Palaeobotany and Palynology*, *58*(2–4), 139–161. https://doi.org/10.1016/0034-6667(89)90082-1

Elmas, A. (2012). The Thrace Basin: Stratigraphic and tectonic-palaeogeographic evolution of the Palaeogene formations of northwest Turkey. *International Geology Review*, *54*(12), 1419–1442. https://doi.org/10.1080/00206814.2011.644732

Elmas, A., Koralay, E., Duru, O., & Schmidt, A. (2016). Geochronology, geochemistry, and tectonic setting of the Oligocene magmatic rocks (Marmaros Magmatic Assemblage) in Gökçeada Island, northwest Turkey. *International Geology Review*, *59*(4), 420–447. https://doi.org/10.1080/00206814.2016.1227941

Erbil, Ü., Okay, A. I., & Hakyemez, A. (2021). Late Oligocene—Early Miocene shortening in the Thrace Basin, northern Aegean. *International Journal of Earth Sciences*, *110*(6), 1921–1936. https://doi.org/10.1007/s00531-021-02047-3

Evenick, J. C. (2021). Glimpses into Earth's history using a revised global sedimentary basin map. *Earth-Science Reviews*, *215*, 103564. https://doi.org/10.1016/j.earscirev.2021.103564

Friedmann, S. J., & Burbank, D. W. (1995). Rift basins and supradetachment basins: Intracontinental extensional end-members. *Basin Research*, *7*(2), 109–127. https://doi.org/10.1111/j.1365-2117.1995.tb00099.x

Georgiev, N., Froitzheim, N., Cherneva, Z., Frei, D., Grozdev, V., Jahn-Awe, S., & Nagel, T. J. (2016). Structure and U–Pb zircon geochronology of an Alpine nappe stack telescoped by extensional detachment faulting (Kulidzhik area, Eastern Rhodopes, Bulgaria). *International Journal of Earth Sciences*, *105*(7), 1985–2012. https://doi.org/10.1007/s00531-016-1293-4

Georgiev, N., Pleuger, J., Froitzheim, N., Sarov, S., Jahn-Awe, S., & Nagel, T. J. (2010). Separate Eocene-early Oligocene and Miocene stages of extension and core complex formation in the western Rhodopes, Mesta basin, and Pirin Mountains (Bulgaria). *Tectonophysics*, *487*(1–4), 59–84. https://doi.org/10.1016/j.tecto.2010.03.009

Geraads, D., Kaya, T., & Mayda, S. (2005). Late Miocene large mammals from Yulafli, Thrace region, Turkey, and their biogeographic implications. *Acta Palaeontologica Polonica*, *50*, 523–544.

Görür, N., & Okay, A. I. (1996). Fore-arc origin of the Thrace basin, northwest Turkey. *Geologische Rundschau*, *85*(4), 662–668. https://doi.org/10.1007/bf02440103

Gürgey, K. (2009). Geochemical overview and undiscovered gas resources generated from Hamitabat petroleum system in the Thrace Basin, Turkey. *Marine and Petroleum Geology*, *26*(7), 1240–1254. https://doi.org/10.1016/j.marpetgeo.2008.08.007

Gürgey, K., & Batı, Z. (2018). Palynological and petroleum geochemical assessment of the lower Oligocene Mezardere Formation, Thrace Basin, NW Turkey. *Turkish Journal of Earth Sciences*, *27*(5), 349–383. https://doi.org/10.3906/yer-1710-24

Gürgey, K., Philp, P., Clayton, C., Emiroglu, H., & Siyako, M. (2005). Geochemical and isotopic approach to maturity/source/mixing estimations for natural gas and associated condensates in the Thrace basin, NW Turkey. *Applied Geochemistry*, *20*(11), 2017–2037. https://doi.org/10.1016/j.apgeochem.2005.07.012

Hejl, E., Bernroider, M., Parlak, O., & Weingartner, H. (2010). Fission-track thermochronology, vertical kinematics, and tectonic development along the western extension of the North Anatolian Fault zone. *Journal of Geophysical Research*, *115*(B10), B10407. https://doi.org/10.1029/2010jb007402

Horstwood, M. S. A., Košler, J., Gehrels, G., Jackson, S. E., McLean, N. M., Paton, C., et al. (2016). Community-derived standards for LA-ICP-MSU-(Th-) Pb geochronology – Uncertainty propagation, age interpretation and data reporting. *Geostandarts and Geoanalytical Research*, *40*(3), 311–332. https://doi.org/10.1111/j.1751-908x.2016.00379.x

Hoşgörmez, H., & Yalçın, M. N. (2005). Gas-source rock correlation in Thrace Basin, Turkey. *Marine and Petroleum Geology*, *22*(8), 901–916. https://doi.org/10.1016/j.marpetgeo.2005.04.002

Huvaz, O., Karahanoglu, N., & Ediger, V. (2007). The thermal gradient history of the Thrace Basin, NW Turkey: Correlation with basin evolution processes. *Journal of Petroleum Geology*, *30*(1), 3–24. https://doi.org/10.1111/j.1747-5457.2007.00003.x

Huvaz, O., Sarikaya, H., & Nohut, Ö. M. (2005). Nature of a regional dogleg pattern in maturity profiles from Thrace Basin, northwestern Turkey: A newly discovered unconformity or a thermal anomaly. *American Association of Petroleum Geologists Bulletin*, *89*(10), 1373–1396. https://doi.org/10.1306/06090505021

İlkışık, M. (1981). Study of the crust in Thrace through the magnetotelluric method (in Turkish). *Istanbul Yerbilimleri*, *2*, 307–319.

Ingersoll, R. V. (2011). Tectonics of sedimentary basins, with revised nomenclature. In C. Busby, & A. Azar (Eds.), (Eds), *Tectonics of sedimentary basins: Recent advances* (pp. 1–43). John Wiley & Sons.

İslamoğlu, Y., Harzhauser, M., Gross, M., Jimenez-Moreno, G., Coric, S., Kroh, A., et al. (2008). From Tethys to eastern Paratethys: Oligocene depositional environments, paleoecology and paleobiogeography of the Thrace Basin (NW Turkey). *International Journal of Earth Sciences*, *99*(1), 183–200. https://doi.org/10.1007/s00531-008-0378-0

Kaiser-Rohrmeier, M., von Quadt, A., Driesner, T., Heinrich, C., Handler, R., Ovtcharova, M., et al. (2013). Post-orogenic extension and hydrothermal ore formation: High precision geochronology of the central Rhodopian metamorphic core complex (Bulgaria-Greece). *Economic Geology*, *108*(4), 691–718. https://doi.org/10.2113/econgeo.108.4.691

Kauffmann, G., Kockel, F., & Mollat, H. (1976). Notes on the stratigraphic and paleogeographic position of the Svoula formation in the innermost zone of the Hellenides (northern Greece). *Bulletin de la Societe Geologique de France*, *18*(2), 225–230. https://doi.org/10.2113/gssgfbull.s7-xviii.2.225

Kaymakci, N., Aldanmaz, E., Langereis, C., Spel, T. L., Gurer, O. F., & Zanetti, K. A. (2007). Late Miocene transcurrent tectonics in NW Turkey: Evidence from paleomagnetism and ^{40}Ar-^{39}Ar dating of alkaline volcanic rocks. *Geological Magazine*, *144*(2), 379–392. https://doi.org/10.1017/s0016756806003074

Kende, J., Henry, P., Bayrakci, G., Özeren, M. S., & Grall, C. (2017). Moho depth and crustal thinning in the Marmara Sea region from gravity data inversion. *Journal of Geophysical Research: Solid Earth*, *122*(2), 1381–1401. https://doi.org/10.1002/2015jb012735

Kilias, A., Falalakis, G., Sfeikos, A., Papadimitriou, E., Vamvaka, A., & Gkarlaouni, C. (2013). The Thrace basin in the Rhodope province of NE Greece — A Tertiary supradetachment basin and its geodynamic implications. *Tectonophysics*, *595–596*, 90–105. https://doi.org/10.1016/j.tecto.2012.05.008

Klepeis, K. A., Crawford, M. L., & Gehrels, G. A. (1998). Structural history of the crustal-scale Coast shear zone near Portland Inlet, SE Alaska and British Columbia. *Journal of Structural Geology*, *20*(7), 883–904. https://doi.org/10.1016/s0191-8141(98)00020-0

Kopp, K. O. (1965). Geologie Thrakiens III: Das Tertiar zwischen Rhodope und Evros. *Annales Geologiques des Pays Helleniques*, *46*, 315–362.

Kopp, K. O., Pavoni, N., & Schindler, C. (1969). Geologie Thrakiens IV: Das Ergene Becken. *Beihefte zum geologischen Jahrbuch*, (76), 136.

Kounov, A., Seward, D., Burg, J. P., Stockli, D., & Wüthrich, E. (2020). Cenozoic thermal evolution of the central Rhodope metamorphic complex (southern Bulgaria). *International Journal of Earth Sciences*, *109*(5), 1589–1611. https://doi.org/10.1007/s00531-020-01862-4

Kounov, A., Wüthrich, E., Seward, D., Burg, J. P., & Stockli, D. (2015). Low-temperature constraints on the Cenozoic thermal evolution of the southern Rhodope core complex (northern Greece). *International Journal of Earth Sciences*, *104*(5), 1337–1352. https://doi.org/10.1007/s00531-015-1158-2

Kylander-Clark, A. R. C., Hacker, B. R., & Cottle, J. M. (2013). Laser-ablation split-stream ICP petrochronology. *Chemical Geology*, *345*, 99–112. https://doi.org/10.1016/j.chemgeo.2013.02.019

Lebküchner, R. F. (1974). Beitrag zur Kenntnis des Geologie des Oligozäns von Mittel Thrakien (Türkei). *Bulletin of the Mineral Research and Exploration*, *83*, 1–30.

Less, G., Özcan, E., & Okay, A. I. (2011). Stratigraphy and larger foraminifera of the Middle Eocene to Lower Oligocene shallow-marine units in the northern and eastern parts of the Thrace Basin, NW Turkey. *Turkish Journal of Earth Sciences*, *20*, 793–845. https://doi.org/10.3906/yer-1010-53

Lips, A. L. W., White, S. H., & Wijbrans, J. R. (2000). Middle-late Alpine thermotectonic evolution of the southern Rhodope Massif, Greece. *Geodinamica Acta*, *13*(5), 281–292. https://doi.org/10.1016/s0985-3111(00)00042-5

Maravelis, A. G., Boutelier, D., Catuneanu, O., Seymour, K. S., & Zelilidis, A. (2016). A review of tectonics and sedimentation in a forearc setting: Hellenic Thrace Basin, north Aegean sea and northern Greece. *Tectonophysics*, *674*, 1–19. https://doi.org/10.1016/j.tecto.2016.02.003

Marchev, P., Jicha, B., Raicheva, R., Ivanova, R., Peytcheva, I., & Grozdev, V. (2020). ^{40}Ar/^{39}Ar and U-Pb ages for 33.3 Ma supereruptions from Bulgaria: Evidence from eastern Rhodopes and Varna Mn mineralizations (Bulgaria) and Lemnos island (Greece). *Review of the Bulgarian Geological Society*, *81*, 87–89.

Márton, I., Moritz, R., & Spikings, R. (2010). Application of low-temperature thermochronology to hydrothermal ore deposits: Formation, preservation and exhumation of epithermal gold systems from the Eastern Rhodopes, Bulgaria. *Tectonophysics*, *483*(3–4), 240–254. https://doi.org/10.1016/j.tecto.2009.10.020

Meinhold, G., & Kostopoulos, D. K. (2013). The Circum-Rhodope belt, northern Greece: Age, provenance, and tectonic setting. *Tectonophysics*, *595–596*, 55–68. https://doi.org/10.1016/j.tecto.2012.03.034

Mueller, M. A., Licht, A., Campbell, C., Ocakoğlu, F., Taylor, M. H., Burch, L., et al. (2019). Collision chronology along the İzmir-Ankara-Erzincan suture zone: Insights from the Sarıcakaya basin, western Anatolia. *Tectonics*, *38*(10), 3652–3674. https://doi.org/10.1029/2019tc005683

Nikishin, A. M., Okay, A. I., Tüysüz, O., Demirer, A., Amelin, N., & Petrov, E. (2015). The Black Sea basins structure and history: New model based on new deep penetration regional seismic data. Part 1: Basin structure and fill. *Marine and Petroleum Geology*, *59*, 638–655. https://doi.org/10.1016/j.marpetgeo.2014.08.017

Okay, A. I. (2023). Geochronological and biostratigraphic data on the Thrace Basin, northwest Turkey [Dataset]. Mendeley V1. https://doi.org/10.17632/hy3s7bm97k.1

Okay, A. I., Kaşlılar-Özcan, A., İmren, C., Boztepe-Güney, A., Demirbağ, E., & Kuşçu, İ. (2000). Active faults and strike slip basins in the Marmara Sea, northwest Turkey: A multi-channel seismic reflection study. *Tectonophysics*, *321*(2), 189–218. https://doi.org/10.1016/s0040-1951(00)00046-9

Okay, A. I., & Kylander-Clark, A. R. C. (2023). No sediment transport across the Tethys Ocean during the latest Cretaceous: Detrital zircon record from the Pontides and the Anatolide-Tauride block. *International Journal of Earth Sciences*, *112*(3), 999–1022. https://doi.org/10.1007/s00531-022-02275-1

Okay, A. I., Özcan, E., Cavazza, W., Okay, N., & Less, G. (2010). Basement types, lower Eocene series, upper Eocene olistostromes and the initiation of the southern Thrace Basin, NW Turkey. *Turkish Journal of Earth Sciences*, *19*, 1–25. https://doi.org/10.3906/yer-0902-10

Okay, A. I., Özcan, E., Hakyemez, A., Siyako, M., Sunal, G., & Kylander-Clark, A. R. C. (2019). The Thrace Basin and the Black Sea: The Eocene - Oligocene connection. *Geological Magazine*, *156*(1), 39–61. https://doi.org/10.1017/s0016756817000772

Okay, A. I., Satır, M., Tüysüz, O., Akyüz, S., & Chen, F. (2001). The tectonics of the Strandja Massif: Variscan and mid-Mesozoic deformation and metamorphism in the northern Aegean. *International Journal of Earth Sciences*, *90*(2), 217–233. https://doi.org/10.1007/s005310000104

Okay, A. I., Topuz, T., Kylander-Clark, A. R. C., Sherlock, S., & Zattin, M. (2022). Late Paleocene – Middle Eocene magmatic flare-up in western Anatolia. *Lithos*, *428–429*, 106816. https://doi.org/10.1016/j.lithos.2022.106816

Okay, A. I., Tüysüz, O., & Kaya, Ş. (2004). From transpression to transtension: Changes in morphology and structure around a bend on the North Anatolian Fault in the Marmara region. *Tectonophysics*, *391*(1–4), 259–282. https://doi.org/10.1016/j.tecto.2004.07.016

Okay, A. I., Zattin, M., Özcan, E., & Sunal, G. (2020). Uplift of Anatolia. *Turkish Journal of Earth Sciences*, *29*(5), 696–713. https://doi.org/10.3906/yer-2003-10

Önal, M. (1986). Sedimentary facies and tectonic evolution of central part of the Gelibolu Peninsula, NW Anatolia, Turkey (in Turkish). *Jeoloji Mühendisliği*, *29*, 37–46. Retrieved from https://www.jmo.org.tr/resimler/ekler/e7f47e09c8e05e6_ek.pdf

Ozansoy, F. (1962). Les anthrocothériens de l'oligocene inférieur de la Thrace orientale (Turquie). *Bulletin of the Mineral Research and Exploration*, *58*, 85–96.

Özcan, E., Less, G., & Kertész, B. (2007). Late Ypresian to Middle Lutetian orthophragminid record from central and northern Turkey: Taxonomy and remarks on zonal scheme. *Turkish Journal of Earth Sciences*, *16*, 281–321.

Özcan, E., Less, G., Okay, A. I., Báldi-Beke, M., Kollányi, K., & Yilmaz, İ. Ö. (2010). Stratigraphy and larger foraminifera of the Eocene shallow-marine and olistostromal units of the southern part of the Thrace Basin, NW Turkey. *Turkish Journal of Earth Sciences*, *19*, 27–77. https://doi.org/10.3906/yer-0902-11

Özcan, E., Okay, A. I., Bürkan, K. A., Yücel, A. O., & Özcan, Z. (2018). The Bartonian-Priabonian marine record of the Biga Peninsula, NW Anatolia (Turkey): Larger benthic foraminifera, revised stratigraphy and implications for the regional geology. *Geológica Acta*, *16*, 163–187.

Özcan, E., Özcan, Z., Okay, A. I., Akbayram, K., & Hakyemez, A. (2020). Ypresian-to Lutetian marine record in NW Turkey: A revised biostratigraphy and chronostratigraphy and implications for the Eocene paleogeography. *Turkish Journal of Earth Sciences*, *29*(SI-1), 1–27. https://doi.org/10.3906/yer-1903-3

Özcan, Z., Okay, A. I., Özcan, E., Hakyemez, A., & Özkan-Altıner, S. (2012). Late Cretaceous - Eocene geological evolution of the Pontides in northwest Turkey between the Black Sea coast and Bursa. *Turkish Journal of Earth Sciences*, *21*, 933–960.

Perinçek, D. (1991). Possible strand of the North Anatolian Fault in the Thrace Basin, Turkey-an interpretation. *American Association of Petroleum Geologists Bulletin*, *75*, 241–257.

Perinçek, D., Ataş, N., Karatut, Ş., & Erensoy, E. (2015). Geological factors controlling potential of lignite beds within the Danişmen Formation in the Thrace Basin. *Bulletin of the Mineral Research and Exploration*, *150*, 77–107. https://doi.org/10.19111/bmre.65462

Robinson, A. G., Rudat, J. H., Banks, C. J., & Wiles, R. L. F. (1996). Petroleum geology of the Black Sea. *Marine and Petroleum Geology*, *13*(2), 195–223. https://doi.org/10.1016/0264-8172(95)00042-9

Sağlam, E., Duzman, T., Ay, C., Okay, A. I., Topuz, G., Sunal, G., et al. (2023). Late Cretaceous arc magmatism in the Western Pontides – Temporal and chemical changes. *International Geology Review*, 1–24. https://doi.org/10.1080/00206814.2023.2221982

Saner, S. (1980). Plate tectonic explanation of the basins in the western Pontides and neighbouring areas, northwest Turkey (in Turkish). *Maden Tetkik ve Arama Dergisi*, *93/94*, 1–19.

Schmidt, A., Pourteau, A., Candan, O., & Oberhänsli, R. (2015). Lu–Hf geochronology on cm-sized garnets using microsampling: New constraints on garnet growth rates and duration of metamorphism during continental collision (Menderes Massif, Turkey). *Earth and Planetary Science Letters*, *432*, 24–35. https://doi.org/10.1016/j.epsl.2015.09.015

Şen, Ş., & Yıllar, S. (2016). Nature, genesis, and significance of the Gazikoy and Kesan formations (Thrace Basin, Turkey): Eocene turbidites and olistostromes formed on an active Tethyan margin. *The Journal of Geology*, *124*(4), 463–479. https://doi.org/10.1086/686629

Şenol, M. (1980). Depositional environment of Oligocene units and lignite formations in the Keşan (Edirne) and Marmara Ereğlisi (Tekirdağ) regions (in Turkish). *Turkiye Jeoloji Kurumu Bulteni*, *23*, 133–140.

Şentürk, K., Sümengen, M., Terlemez, İ., & Karaköse, C. (1998). *Geological map and explanatory notes, Çanakkale-D4 sheet, (scale 1:100 000)*. Maden Tetkik ve Arama Genel Müdürlüğü.

Simmons, M. D., Bidgood, M. D., Connell, P. G., Coric, S., Okay, A. I., Shaw, D., et al. (2020). Biostratigraphy and paleoenvironments of the Oligocene succession (İhsaniye formation) at Karaburun (NW Turkey). *Turkish Journal of Earth Sciences*, *29*(SI-1), 28–63. https://doi.org/10.3906/yer-1907-7

Sinclair, H. D., Juranov, S. G., Georgiev, G., Byrne, P., & Mountney, N. P. (1997). The Balkan thrust wedge and foreland basin of eastern Bulgaria: Structural and stratigraphic development. In A. G. Robinson (Ed.), *Regional and Petroleum geology of the Black Sea and surrounding region* (pp. 91–114). American Association of Petroleum Geologists Memoir. No. 68.

Siyako, M. (2006a). "Lignitic sandstones" of the Trakya basin. *Bulletin of the Mineral Research and Exploration*, *132*, 63–72.

Siyako, M. (2006b). Tertiary rock units of the Thrace Basin (in Turkish). In *Lithostratigraphic units of the Thrace region* (pp. 55–83). Maden Tetkik ve Arama Genel Müdürlüğü.

Siyako, M., & Huvaz, O. (2007). Eocene stratigraphic evolution of the Thrace Basin, Turkey. *Sedimentary Geology*, *198*(1–2), 75–91. https://doi.org/10.1016/j.sedgeo.2006.11.008

Sláma, J., Košler, J., Condon, D. J., Crowley, J. L., Gerdes, A., Hanchar, J. M., et al. (2008). Plešovice zircon-a new natural reference material for U-Pb and Hf isotopic microanalysis. *Chemical Geology*, *249*(1–2), 1–35. https://doi.org/10.1016/j.chemgeo.2007.11.005

Speijer, R. P., Pälike, H., Hollis, C. J., Hooker, J. J., & Ogg, J. G. (2020). The Paleogene period. In F. M. Gradstein, J. G. Ogg, M. D. Schmitz, & G. M. Ogg (Eds.), *Geologic time scale 2020* (pp. 1087–1140). Elsevier.

Steininger, F. F., & Wessely, G. (2000). From the Tethyan Ocean to the Paratethys sea: Oligocene to Neogene stratigraphy, paleogeography and paleobiogeography of the circum-Mediterranean region and the Oligocene to Neogene basin evolution in Austria. *Mitteilungen der Osterreichischen Geologischen Gesellschaft*, *92*, 95–116.

Sümengen, M., & Terlemez, I. (1991). Stratigraphy of the Eocene sediments from the southwestern Thrace. *Bulletin of the Mineral Research and Exploration*, *113*, 15–29.

Sunal, G., Satır, M., Natal'in, B., Topuz, G., & von der Scmidt, O. (2011). Metamorphism and diachronous cooling in a contractional orogen: The Strandja Massif, NW Turkey. *Geological Magazine*, *148*(4), 580–596. https://doi.org/10.1017/s0016756810001020

Topuz, G., Okay, A. I., Altherr, R., Satir, M., & Schwarz, W. H. (2008). Late Cretaceous blueschist-facies metamorphism in southeastern Thrace (Turkey) and its geodynamic implications. *Journal of Metamorphic Geology*, *26*(9), 895–913. https://doi.org/10.1111/j.1525-1314.2008.00792.x

Turgut, S., & Eseller, G. (2000). Sequence stratigraphy, tectonics and depositional history in Eastern Thrace Basin, NW Turkey. *Marine and Petroleum Geology*, *17*(1), 61–100. https://doi.org/10.1016/s0264-8172(99)00015-x

Turgut, S., Türkarslan, M., & Perinçek, D. (1991). Evolution of the Thrace sedimentary basin and its hydrocarbon prospectivity. In A. M. Spencer (Ed.), *Generation, accumulation, and production of Europe's hydrocarbons* (pp. 415–437). Special Publication of the European Association of Petroleum Geoscientists. No. 1.

Türkecan, A., & Yurtsever, A. (2002). *Geological map series of Turkey, Istanbul sheet (scale 1: 500 000)*. Maden Tetkik ve Arama Genel Müdürlüğü.

Türkoğlu, E., Zulauf, G., Linckens, J., & Ustaömer, T. (2016). Dextral strike-slip along the Kapıdağ shear zone (NW Turkey): Evidence for Eocene westward translation of the Anatolian plate. *International Journal of Earth Sciences*, *105*(7), 2061–2073. https://doi.org/10.1007/s00531-016-1372-6

Turpaud, P., & Reischmann, T. (2010). Characterisation of igneous terranes by zircon dating: Implications for UHP occurrences and suture identification in the central Rhodope, northern Greece. *International Journal of Earth Sciences*, *99*(3), 567–591. https://doi.org/10.1007/s00531-008-0409-x

Ünay, E., & de Bruijn, H. (1984). On some rodent assemblages from both sides of the Dardanelles, Turkey. *Newsletter in Stratigraphy*, *13*(3), 119–132. https://doi.org/10.1127/nos/13/1984/119

Ünay-Bayraktar, E. (1989). *Rodents from the middle Oligocene of Turkish Thrace*. Utrecht Micropaleontological Bulletins, Special Publication (No. (5), p. 120)).

Ustaömer, P. A., Ustaömer, T., Collins, A. S., & Reischpeitsch, J. (2009). Lutetian arc-type magmatism along the southern Eurasian margin: New U-Pb LA-ICPMS and whole rock geochemical data from Marmara Island, NW Turkey. *Mineralogy and Petrology*, *96*(3–4), 177–196. https://doi.org/10.1007/s00710-009-0051-8

Wade, B. S., Pearson, P. N., Berggren, W. A., & Pälike, H. (2011). Review and revision of Cenozoic tropical planktonic foraminiferal biostratigraphy and calibration to the geomagnetic polarity and astronomical time scale. *Earth-Science Reviews*, *104*(1–3), 111–142. https://doi.org/10.1016/j.earscirev.2010.09.003

Wawrzenitz, N., Krohe, A., Baziotis, I., Mposkos, E., Kylander-Clark, A., & Romer, R. L. (2015). LASS U-Th-Pb monazite and rutile geochronology of felsic high-pressure granulites (Rhodope, N Greece): The role of fluids, deformation and metamorphic reactions. *Lithos*, *232*, 266–285. https://doi.org/10.1016/j.lithos.2015.06.029

Xie, X., & Heller, P. L. (2009). Plate tectonics and basin subsidence history. *Geological Society of America Bulletin*, *121*, 55–64.

Yıldız, A., Toker, V., & Şengüler, İ. (1997). The nannoplankton biostratigraphy of the Middle Eocene-Oligocene units in southern Thrace basin and the surface water temperature variations. *Türkiye Petrol Jeologları Derneği Bülteni*, *9*, 31–44.

Yücel, A. O., Özcan, E., & Erbil, Ü. (2020). Latest Priabonian larger benthic foraminiferal assemblages at the demise of the Soğucak carbonate platform (Thrace Basin and Black Sea shelf, NW Turkey): Implications for the shallow marine biostratigraphy. *Turkish Journal of Earth Sciences*, *29*(SI-1), 85–114. https://doi.org/10.3906/yer-1904-19

Zattin, M., Cavazza, W., Okay, A. I., Federici, I., Fellin, M. G., Pignalosa, A., & Reiners, P. (2010). A precursor of the North Anatolian Fault in the Marmara Sea region. *Journal of Asian Earth Sciences*, *39*(3), 97–108. https://doi.org/10.1016/j.jseaes.2010.02.014

Zattin, M., Okay, A. I., & Cavazza, W. (2005). Fission-track evidence for late Oligocene and mid-Miocene activity along the North Anatolian Fault in southwestern Thrace. *Terra Nova*, *17*(2), 95–101. https://doi.org/10.1111/j.1365-3121.2004.00583.x